X-551-72-202

PREPRINT

NASA TM X- 65955

SENSOR LIGHTING CONSIDERATIONS FOR EARTH OBSERVATORY SATELLITE MISSIONS

J. L. COOLEY

JUNE 1972

GSFC — GODDARD SPACE FLIGHT CENTER —

GREENBELT, MARYLAND

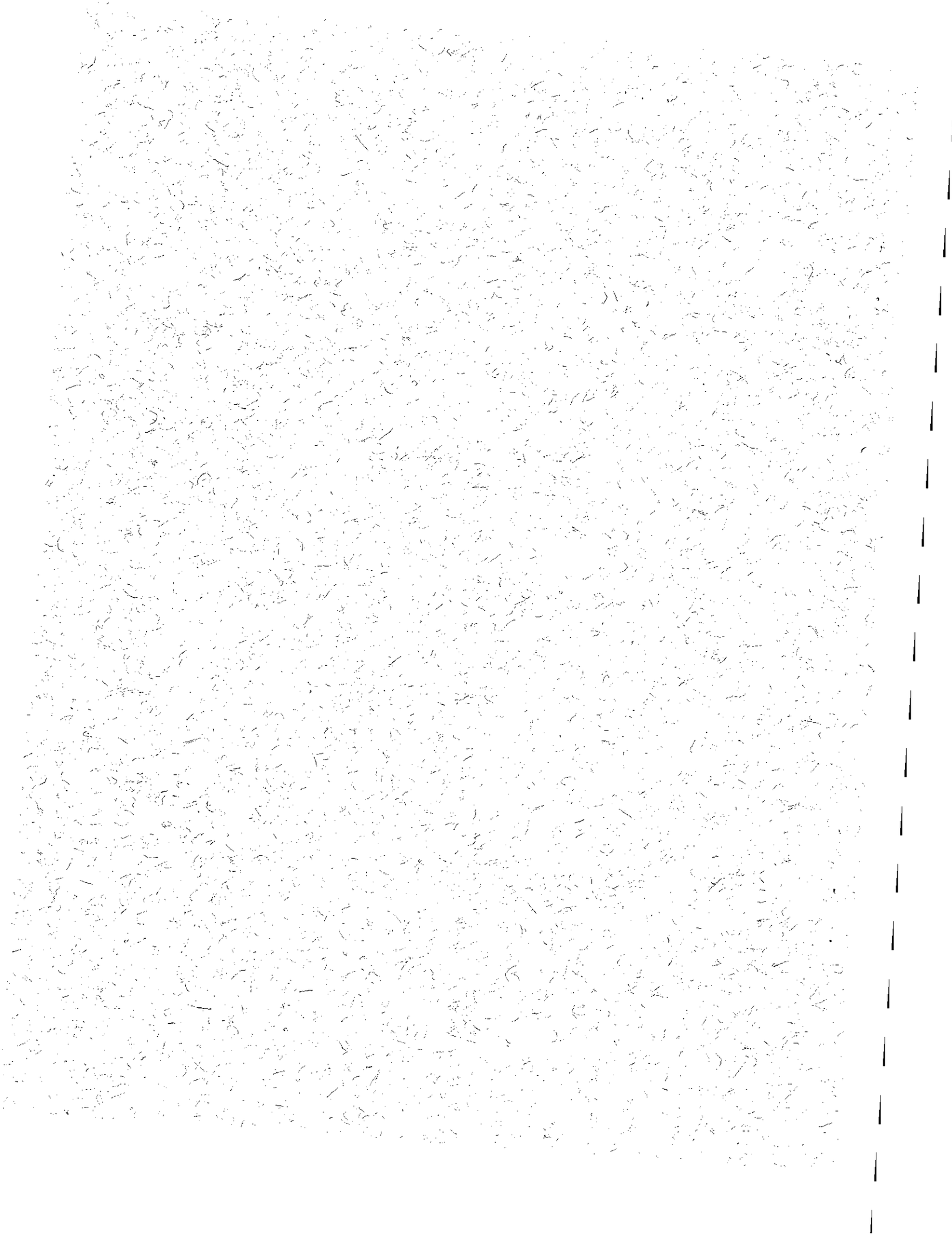

X-551-72-202
PREPRINT

SENSOR LIGHTING CONSIDERATIONS FOR EARTH OBSERVATORY SATELLITE MISSIONS

J. L. Cooley

June 1972

GODDARD SPACE FLIGHT CENTER
Greenbelt, Maryland

SENSOR LIGHTING CONSIDERATIONS FOR EARTH OBSERVATORY SATELLITE MISSIONS

J. L. Cooley

ABSTRACT

This report considers several facets of sensor lighting conditions for Earth observatory satellite missions. Assuming onboard sensors of a given width (5°, 10°, 20°, 30°, 52°, or horizon sensor width angle) viewing perpendicular to the subsatellite ground track along sun-synchronous orbits with various nodes (giving 6 A.M. to 6 P.M. equator crossings), the ground trace of the ends of the sensor coverage are found and the variation in solar illumination on the ground across the line covered by the sensor is found during the day for any point along the orbit. Also the changes with season and variation during the year are found. In some cases one end of a horizon sensor is almost continuously in sunlight during the year, while the other end is almost continuously in darkness (this occurs for 6 A.M. or 6 P.M. orbits). Also certain glint points, where the sun's rays are reflected exactly at the spacecraft, the glint trace, and points along the orbit where glint might seriously affect a sensor (occurring between a subsatellite latitude of 38-1/2 degrees north and 38-1/2 degrees south for the cases considered) are found. With this information, the expected lighting conditions will be known for a given sensor for various Earth observatory satellite orbits.

CONTENTS

ILLUSTRATIONS

ILLUSTRATIONS (continued)

ILLUSTRATIONS (continued)

SENSOR LIGHTING CONSIDERATIONS FOR EARTH OBSERVATORY SATELLITE MISSIONS

INTRODUCTION

There are a variety of possible orbits for Earth observatory satellite missions. These orbits have different altitudes and repeat cycle periods, and give different ground tracks and ground trace patterns. Various ground trace patterns for orbits with 16 day, 17 day, and 18 day repeat cycles are discussed in Reference 1. Certain ground trace patterns optimize the information from various onboard sensors - for example, from a thematic mapper having a 185 km. ground swath, or an oceanic imaging spectrophotometer with a 740 km. ground swath, or several types of radiometers having horizon to horizon scanning capability. Thus the orbit selection process is intimately related to the sensor selection process.

Another way that the orbit selection process interfaces with sensor development and selection is through consideration of sensor lighting conditions to be met on a given orbit. This report considers several facets of sensor lighting conditions for Earth observatory satellite missions. A particular 13-13/17 sun-synchronous orbit is chosen (see Reference 1) with the node allowed to vary. Assuming an onboard sensor of a given width (5°, 10°, 20°, 30°, 52°, or horizon width) viewing perpendicular to the subsatellite ground track, the ends of the sensor coverage produce their own ground trace and there is a variation in solar illumination across the sensor coverage from one end to the other. The goal of this report is to determine the variation in sun elevation angles for sensors of various widths for various nodes (ascending and descending in daylight, from 6 A.M. to 6 P.M., for each equinox and solstice during the year). Also, there may be points where sun glint is a problem; that is, where the sun's rays reflect off a smooth surface to the spacecraft — thereby making a sensor less effective. The goal of this paper is also to determine the glint points and glint trace during the year. With this information, the expected lighting conditions will be known for a given sensor on any chosen orbit.

VARIATION OF LIGHTING FOR VARIOUS SENSOR WIDTHS

This section will display the equations to translate a line sensor width into the sublatitude and sublongitude points at the ends of the sensor coverage. Then from any latitude and longitude point on the Earth's surface at a given time, the sun elevation angle may be calculated. In this way the time history of the lighting conditions across sensors of various widths may be found for various orbits and nodes.

A 13-13/17 circular sun-synchronous orbit will be used as an example of an Earth observatory satellite orbit (see Reference 1). Various nodes will be looked at, from 6 A.M. to 6 P.M. in 2-hour intervals, with both ascending node and descending node in daylight. Each of the 4 seasons, at the equinoxes and solstices, will also be considered. Then there are 7 times of day, 2 types of nodes, and 4 seasons — or 56 possible cases to consider.

Modifications were made to the SANDTRACKS world map and look angle computer program (Reference 2). This program previously computed the subsatellite latitude and longitude points, and gave the sun elevation angles beneath the spacecraft. Additions were made to determine the latitude and longitude points covered by various width line sensors, and to compute the lighting conditions across a line sensor at any time.

A Horizon Sensor

Consider the following figure:

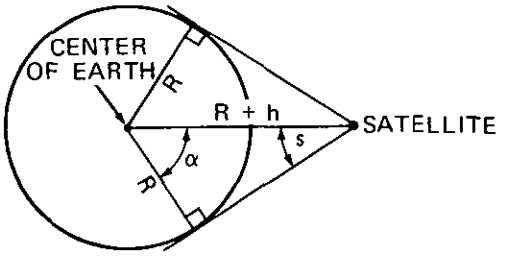

To have the horizon visible from a satellite at a given instant requires:

$$\alpha = \cos^{-1}\left(\frac{R}{R+h}\right)$$

and

$$s = \sin^{-1}\left(\frac{R}{R+h}\right)$$

where

R = earth radius (equatorial radius = 6378km).

α = central angle between the subsatellite point and the outer edge of the area visible from the satellite.

h = altitude of the satellite (976 km for a 13-13/17 orbit).

s = spacecraft sensor width angle.

Then

$$s = \sin^{-1}\left(\frac{R}{R+h}\right) = \sin^{-1}\left(\frac{6378}{7354}\right) = 60.144°$$

and

$$\alpha = 29.856°.$$

Thus a 60.144 degree width sensor onboard an Earth observatory spacecraft in a 13-13/17 orbit will have visibility to the Earth horizon. In that case the coverage central angle will be 29.856 degrees.

The coverage arc length is given by:

$$d = R\alpha = (6378\,\text{km})\ (0.521\ \text{radians}) = 3323.5\ \text{kilometers}.$$

Assuming visibility over 360 degrees, the percent of the Earth's surface area visible from the satellite is:

$$\text{Area} = \frac{2\pi R^2\ (1 - \cos\alpha)}{4\pi R^2} = \left[\frac{1 - \cos\alpha}{2}\right] \times 100\% = 6.64\%.$$

Coverage Half-Angles for Various Sensor Widths

Given a spacecraft sensor width angle s, the central angle α may be determined. Define γ in the following figure:

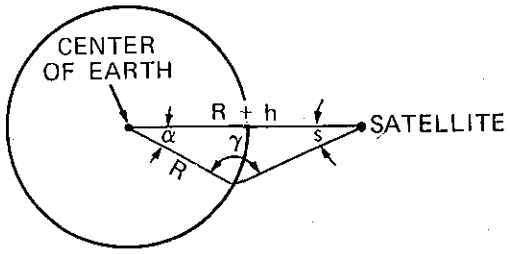

Then,

$$\frac{R + h}{\sin \gamma} = \frac{R}{\sin s}$$

or

$$\sin \gamma = \frac{R + h}{R} \sin s = 1.153 \sin s$$

When s is given, γ may be computed and since $\alpha + \gamma + s = 180°$, then α may be found by the formula $\alpha = 180° - \gamma - s$.

Note that γ is between 90 and 180 degrees. When the computer gives a value for the arc sin such that $0 \leq \gamma < 90°$, the computer is actually producing $\gamma^1 = 180° - \gamma$, so that $\alpha = \gamma^1 - s$.

Sensor width angles of 5, 10, 20, 30, 52, and horizon width (60.144) in degrees will be considered. For these sensor width angles the corresponding coverage half-angles are given below:

Sensor width angle s	Coverage half-angle α
5°	0.768°
10°	1.550°
20°	3.226°
30°	5.206°
52°	13.312°
60.144° (horizon)	29.856°

Perimeter Area Coverage

It is necessary to relate the coverage information, given in terms of sensor width angle s, to geocentric longitude and latitude on the Earth's surface. This can be done via a formulation given in the Orbital Flight Handbook (Reference 3).

Assume that at a certain time the subsatellite point is located at geocentric longitude Ω_0 and geocentric latitude L_0. Let (L, Ω) be a point on the perimeter to be determined:

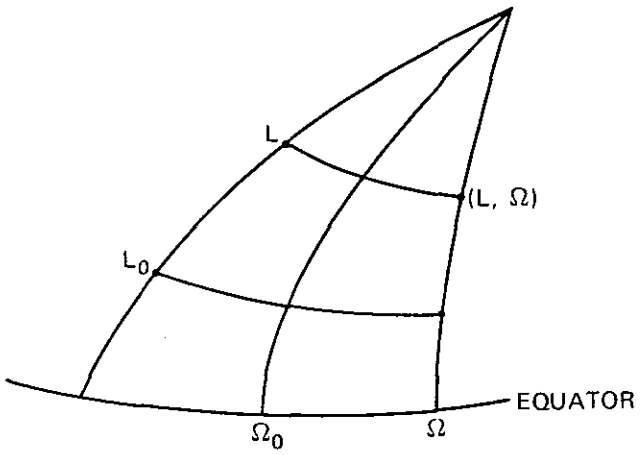

The circular perimeter of the spherical segment of half-angle α (the area in view of the satellite with a sensor width angle s giving a coverage half-angle α) may be determined as:

$$\Omega = \Omega_0 + \Delta\Omega \text{ with } \sin \Delta\Omega = \frac{\sin \alpha \sin \beta}{\cos L}$$

$$\sin L = \sin L_0 \cos \alpha + \cos L_0 \sin \alpha \cos \beta$$

with

Ω_0 = geocentric longitude of subsatellite point

L_0 = geocentric latitude of subsatellite point

α = coverage half-angle (based upon spacecraft sensor width)

β = arbitrary azimuth angle (the parameter of the perimeter solution)

(L, Ω) = a point on the perimeter of the spherical segment about (L_0, Ω_0) of half-angle α

These equations then give a solution for the perimeter of the instantaneous coverage area in terms of the parameter β, the coverage half-angle α, and the geocentric longitude and latitude of the subsatellite point (Ω_0, L_0).

This is shown on the following figure:

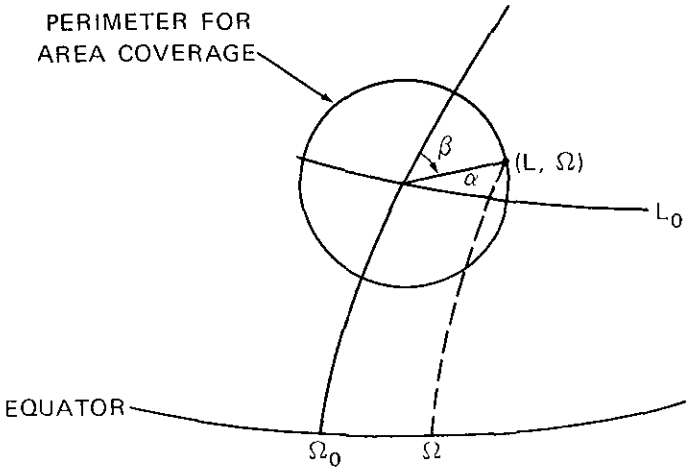

Line Coverage Perpendicular to the Ground Track

The instantaneous perimeter for the coverage available from a satellite with a given sensor width has been found. It is now necessary to determine the two perimeter points perpendicular to the ground track. To get the points perpendicular to the ground track, the orbital inclination then enters the problem, as shown in the following figure:

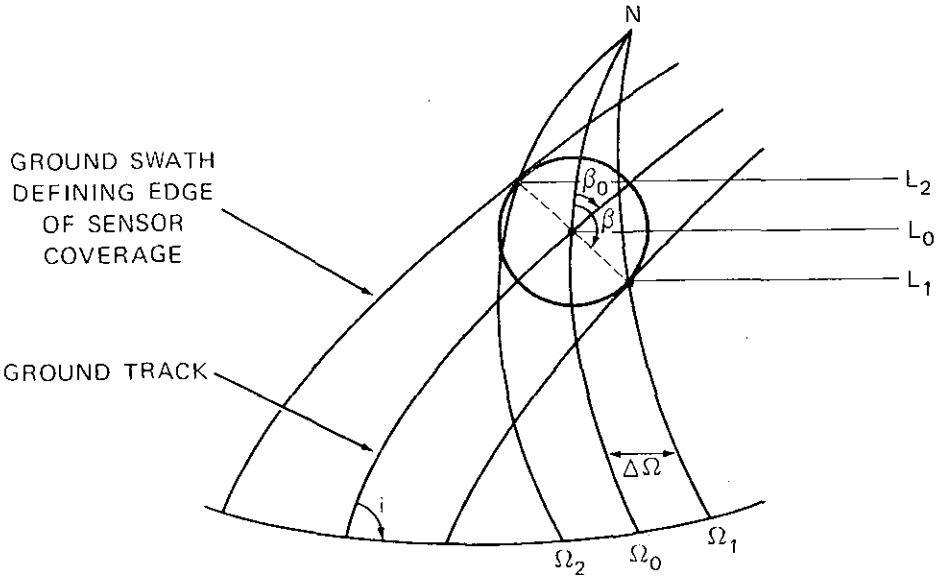

The position of the subsatellite point in geocentric coordinates at a certain time is given by (L_0, Ω_0). The locus of points defining the perimeter of the area covered was given in the previous section. The problem here is to define β such that the two points on the ground swath edges, (L_1, Ω_1) and (L_2, Ω_2), perpendicular to the ground track are determined. The two points are those at the intersections of the circular perimeter and the major circle through (L_0, Ω_0) and perpendicular to the ground track. The two intersection points may be determined by solving for two particular values of β, $\beta = \beta_0 \pm 90°$, where β_0 is the orbit azimuth angle relative to the rotating earth. Now approximately,

$$\sin \beta_0 = \frac{\cos i}{\cos L_0} .$$

Thus given the inclination of the orbit and the subsatellite latitude, the angle β_0 may be calculated. A small correction $\Delta\beta$ may be made to β_0 to correct for rotation of the earth (i.e., to change the orbit azimuth angle in inertial space to an orbit azimuth angle relative to the rotating earth). Now, substituting $\beta = \beta_0 \pm 90°$ in the equations of the previous section gives:

$$\sin L = \sin L_0 \cos \alpha \mp \cos L_0 \sin \alpha \sin \beta_0$$

$$\sin \Delta\Omega = \pm \frac{\sin \alpha \cos \beta_0}{\cos L}$$

These equations then provide two points on the ground swath edges, and the complete ground swath trace may be generated for sets of values (L_0, Ω_0) generated from the ground track solutions.

Summary of Calculations to Determine Latitude and Longitude Points

Given:

$i \equiv$ satellite inclination (99.37 degrees for a 13-13/17 orbit).

$\alpha \equiv$ coverage half-angle, based upon sensor width (found from the previous section for various sensor width angles specified).

Finding a point on the ground trace:

$L_0 \equiv$ subsatellite latitude in geocentric coordinates at a certain time (computed from a world map program, such as SANDTRACKS — Reference 2).

Ω_0 ≡ subsatellite longitude in geocentric coordinates at a certain time (computed from a world map program, such as SANDTRACKS).

From these parameters the latitude (L) and longitude (Ω) points at the edges of the sensor coverage, where the line sensor coverage is perpendicular to the ground track, is found from the calculations:

$$\sin \beta_0 = \cos i / \cos L_0$$

$$\cos \beta_0 = \sqrt{1 - \sin^2 \beta_0}$$

For the first latitude and longitude pair:

$$\sin L_1 = \sin L_0 \cos \alpha - \cos L_0 \sin \alpha \sin \beta_0$$

$$\cos L_1 = \sqrt{1 - \sin^2 L_1}$$

$$L_1 = \sin^{-1} (\sin L_1)$$

$$\sin \Delta\Omega_1 = \frac{\sin \alpha \cos \beta_0}{\cos L_1}$$

$$\Delta\Omega_1 = \sin^{-1} (\sin \Delta\Omega_1)$$

$$\Omega_1 = \Omega_0 + \Delta\Omega_1$$

For the second latitude and longitude pair:

$$\sin L_2 = \sin L_0 \cos \alpha + \cos L_0 \sin \alpha \sin \beta_0$$

$$\cos L_2 = \sqrt{1 - \sin^2 L_2}$$

$$L_2 = \sin^{-1} (\sin L_2)$$

$$\sin \Delta\Omega_2 = - \frac{\sin \alpha \cos \beta_0}{\cos L_2}$$

$$\Delta\Omega_2 = \sin^{-1} (\sin \Delta\Omega_2)$$

$$\Omega_2 = \Omega_0 + \Delta\Omega_2$$

Then the two points on the ground swath edges are found as (L_1, Ω_1) and (L_2, Ω_2).

These equations must be used with caution on a computer, since (1) the longitude increment $\Delta\Omega$ might be greater than 90° in magnitude near the polar regions, whereas the function $\sin^{-1}$ would give a value between 0 and 90°, (2) sensor viewing over a pole causes the longitude to change by 180°, and (3) along an orbit near the pole a sensor switches from looking eastward to looking westward, and vice versa, which must be accounted for by program logic.

Examples for Various Width Sensors

Assume a subsatellite point on the equator for a 13-13/17 ascending node orbit. The ends of the line coverage perpendicular to the orbit for various width sensors are given in the following:

A. 5° width sensor

$s = 5°$ then $\alpha = 0.768°$

$i = 99.37°$

$L_0 = \Omega_0 = 0°$

$\sin \beta_0 = -0.1628$

$\cos \beta_0 = 0.9867$

$\sin L = 0.0022$

$\cos L = 0.9999$

$L = 0.125°$

$\sin \Delta\Omega = 0.0132$

$\Omega = \Delta\Omega = 0.757°$

The ends of the sensor coverage for a 5° width sensor are located at (Lat = 0.125°, Long = 0.757°) and (Lat = -0.125°, Long = -0.757°).

B. 10° width sensor

$s = 10°$ then $\alpha = 1.550°$

$\sin L = 0.0044$

$L = 0.252°$

$$\sin \Delta\Omega = 0.0267$$

$$\Omega = \Delta\Omega = 1.529°$$

The ends of the sensor coverage for a 10° width sensor are located at (Lat = 0.252°, Long = 1.529°) and (Lat = -0.252°, Long = -1.529°).

C. 20° width sensor

$$s = 20° \quad \text{then} \quad \alpha = 3.226°$$

$$\sin L = 0.0092$$

$$L = 0.525°$$

$$\sin \Delta\Omega = 0.0555$$

$$\Omega = \Delta\Omega = 3.183°$$

The ends of the sensor coverage for a 20° width sensor are located at (Lat = 0.525°, Long = 3.183°) and (Lat = -0.525°, Long = -3.183°).

D. 30° width sensor

$$s = 30° \quad \text{then} \quad \alpha = 5.206°$$

$$\sin L = 0.0148$$

$$L = 0.846°$$

$$\sin \Delta\Omega = 0.0895$$

$$\Omega = \Delta\Omega = 5.137°$$

The ends of the sensor coverage for a 30° width sensor are located at (Lat = 0.846°, Long = 5.137°) and (Lat = -0.846°, Long = -5.137°).

E. 52° width sensor

$$s = 52° \quad \text{then} \quad \alpha = 13.312°$$

$$\sin L = 0.0375$$

$$L = 2.148°$$

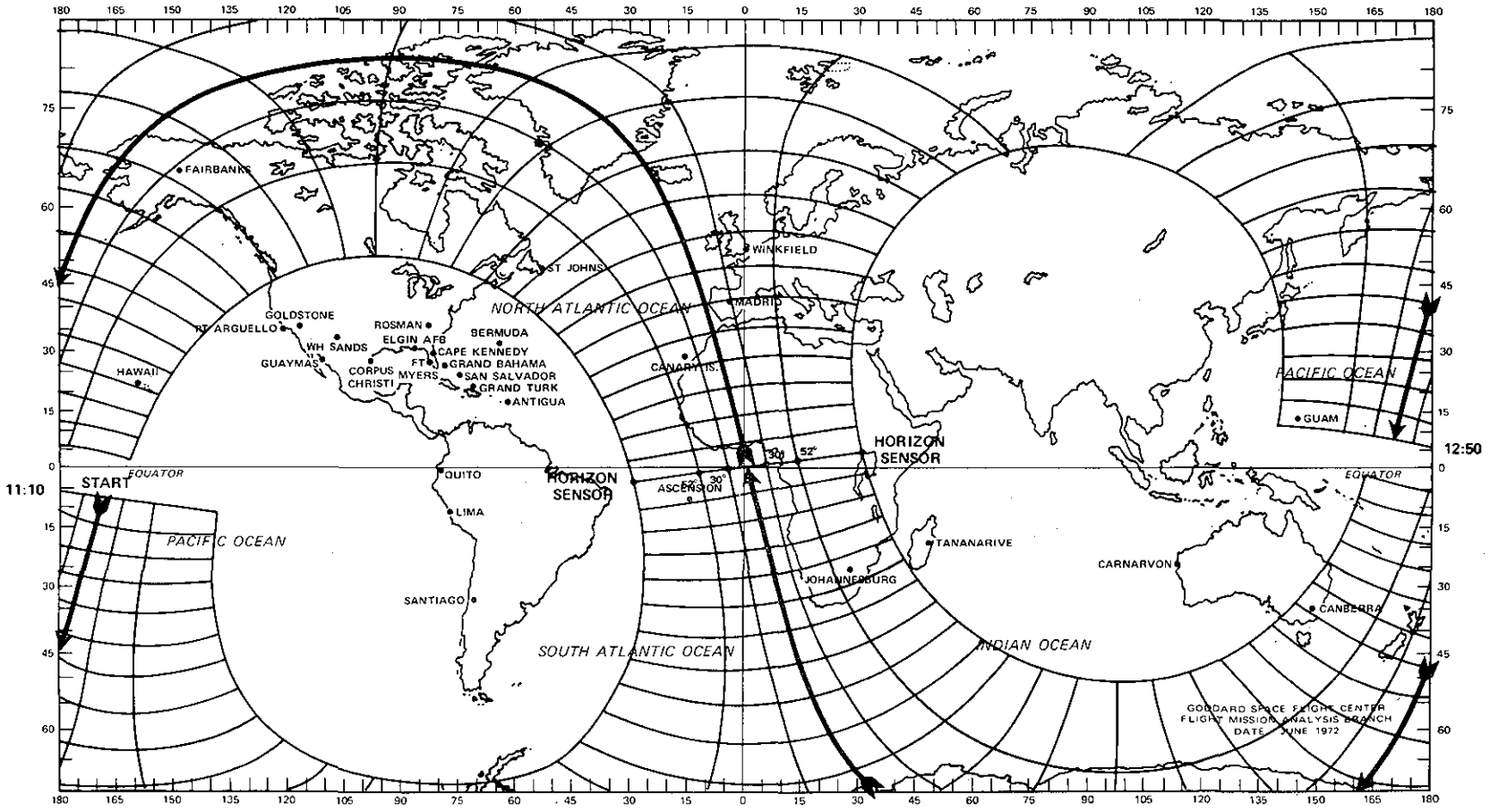

Figure 1. Subsatellite Ground Track and Sensor Ground Track (Ascending Node)

$$\sin \Delta\Omega = 0.2274$$

$$\Omega = \Delta\Omega = 13.141°$$

The ends of the sensor coverage for a 52° width sensor are located at (Lat = 2.148°, Long = 13.141°) and (Lat = -2.148°, Long = -13.141°).

F. 60.144° width horizon sensor

$$s = 60.144° \quad \text{then} \quad \alpha = 29.856°$$

$$\sin L = 0.0810$$

$$L = 4.649°$$

$$\sin \Delta\Omega = 0.4928$$

$$\Omega = \Delta\Omega = 29.53°$$

The ends of the sensor coverage for a horizon width sensor are located at (Lat = 4.649°, Long = 29.53°) and (Lat = -4.649°, Long = -29.53°).

Subsatellite Ground Track and Sensor Ground Swath

The previous equations have been incorporated into the SANDTRACKS world map and look angle computer program. World maps were then generated for 13-13/17 ascending and descending node Earth observatory satellite trajectories, and the ground swaths defining the edges of sensor coverage for a 30°, 52°, and horizon sensor determined. Figures 1 and 2 present this information for one orbit. For the ascending node case in Figure 1, at 11:10 A.M., the orbit proceeds southward to the polar region, at 12 noon the orbit crosses the equator from south-to-north and then proceeds to its maximum northern latitude, and at 12:50 is once again approaching the equator. The sensor ground swath may be followed along continuously for each sensor. The ground trace is given at 2 minute intervals. The sensors less than 30 degrees in width fall between the orbit and the 30° sensor line.

Of particular interest is the nature of the horizon sensor. Following the ground track will explain characteristics of the sun elevation angles, given in the following sections, especially for the 6 A.M. and 6 P.M. nodes. Of interest also is the sensor coverage at and over the polar regions. These 2 figures will be useful in interpreting some of the sun elevation angle behavior for various sensors given in the following figures.

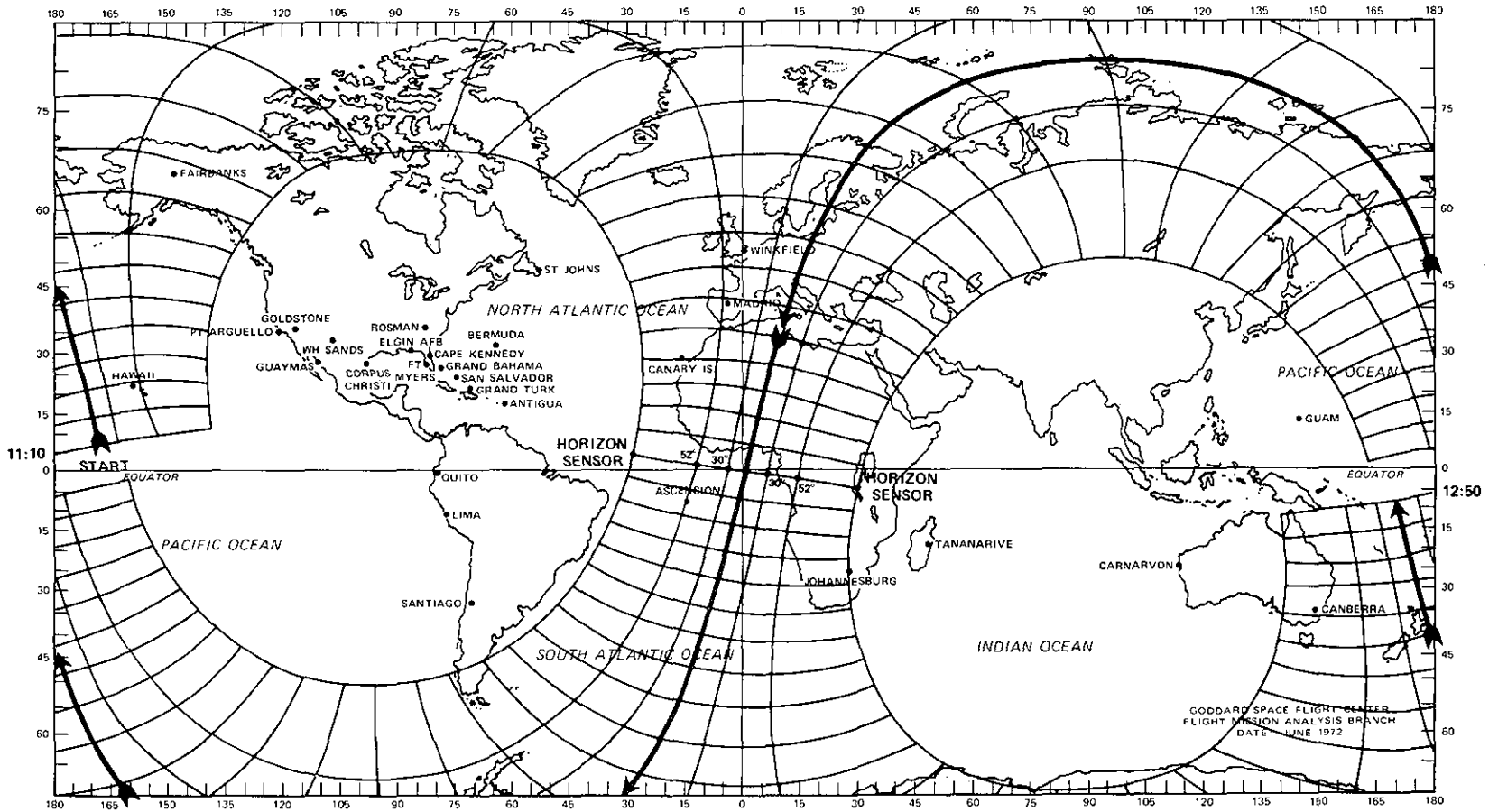

Figure 2. Subsatellite Ground Track and Sensor Ground Track (Descending Node)

Sensor Illumination Considerations

Figures 3 through 23 give a time history of the sun elevation angle across sensors of various widths (5°, 10°, 20°, 30°, 52°, and a horizon sensor) at each of the 4 equinoxes and solstices.

The latitude and longitude points of the sensor ends are given in Figures 1 and 2. The subsolar latitude and longitude points may be placed on these figures for any orbit. For a morning node the sun's position is east of the subsatellite equator crossing (by 30 degrees for a 10 A.M. orbit, 60 degrees for an 8 A.M. orbit, and 90 degrees for a 6 A.M. orbit). For an afternoon orbit the sun's position is west of the subsatellite equator crossing (by 30 degrees for a 2 P.M. orbit, 60 degrees for a 4 P.M. orbit, and 90 degrees for a 6 P.M. orbit). At the vernal equinox (March 21) and autumnal equinox (September 21) the subsolar latitude is 0 degrees. At the summer solstice (June 21) the subsolar latitude is approximately 23.5 degrees north. At the winter solstice (December 21) the subsolar latitude is approximately 23.5 degrees south. Placing the sun in relation to the sensor end points in Figures 1 and 2 makes it easier to interpret the sun elevation angles at the sensor ends for an orbit given in Figures 3 through 23.

Figure 3 gives the sun elevation angles for the various sensors for the ascending node 6 A.M. orbit at the vernal equinox. Figure 1 gives the subsatellite ground track and sensor ground swath for the ascending node orbit; for the 6 A.M. orbit at the vernal equinox the sun is 90 degrees east of the orbit at the equator crossing (subsatellite longitude of approximately 0 degrees, subsolar longitude of approximately 90 degrees east). Then the subsatellite trace in the southern hemisphere is much closer to the sun than in the northern hemisphere. That is shown in Figure 3 where the subsatellite points in the southern hemisphere, but not the northern hemisphere, receive solar illumination. The curves nearest the subsatellite curve on Figure 3 are for the ends of the 5° sensor, the next curves are for the ends of the 10° sensor, and so on for the 20°, 30°, 52°, and horizon sensor ends. An interesting phenomena occurs for this 6 A.M. ascending vernal equinox orbit. The 52° and horizon sensor ends farthest from the sun receive no solar illumination (i.e., are in darkness) while the 52° and horizon sensor ends nearest to the sun are continually in sunlight through the entire orbit. Reviewing Figure 1 shows why this should be so. The maximum solar elevation angle however at any point in the orbit for any sensor is 39 degrees. Figure 3 actually shows 4 cases. Besides the 6 A.M. ascending vernal equinox orbit, it also represents the situation for the 6 A.M. ascending autumnal equinox orbit where the sun is again over the equator, and the 6 P.M. descending node cases for the vernal equinox and autumnal equinox. In the latter 2 cases however the figure must be read from right to left since the orbit trace

proceeds from north to south in the daylight portion of the orbit (see Figure 2 for the ground-trace).

The figures allow for several types of comparisons. Figures 3 - 9 display sun elevation angles for the ascending vernal equinox, 6 A.M., 8 A.M., 10 A.M., Noon, 2 P.M., 4 P.M., and 6 P.M. orbits, respectively. The morning orbits favor the southern hemisphere, the noon orbit is symmetric, and the afternoon orbits favor the northern hemisphere. The variation in maximum solar elevation angle is also shown. Figures 3 - 9 also display sun elevation angles for the descending vernal equinox, 6 P.M., 4 P.M., 2 P.M., Noon, 10 A.M., 8 A.M., and 6 A.M. orbits, respectively. Figures 3 - 9 also show the autumnal equinox ascending and descending cases.

Figures 10 - 16 display sun elevation angles for the ascending summer solstice, 6 A.M., 8 A.M., 10 A.M., Noon, 2 P.M., 4 P.M., and 6 P.M. orbits, respectively. At the summer solstice the latitude of the sun is approximately 23.5 degrees north. Comparing Figures 3 - 9 with Figures 10 - 16 shows a considerable shift in favor of the northern latitude. The maximum solar elevation angle is usually higher and occurs at a more northernly sublatitude point. Figures 10 - 16 also show the winter solstice descending node cases, which however favor the southern hemisphere.

Figures 17 - 23 display sun elevation angles for the descending summer solstice, 6 A.M., 8 A.M., 10 A.M., Noon, 2 P.M., 4 P.M., and 6 P.M. orbits, respectively. The northern hemisphere is even more heavily favored in these cases. Figures 17 - 23 also show the winter solstice ascending node cases, which however heavily favor the southern hemisphere.

The variations throughout a year may also be followed from these figures. Take the 6 A.M. ascending node orbits. The solar elevation angles for the vernal equinox are given on Figure 3, for the summer solstice on Figure 10, autumnal equinox on Figure 3, and winter solstice on Figure 17. The shifts favoring the northern or southern hemispheres, and the changes in magnitude of the solar elevation angles may be followed throughout the year.

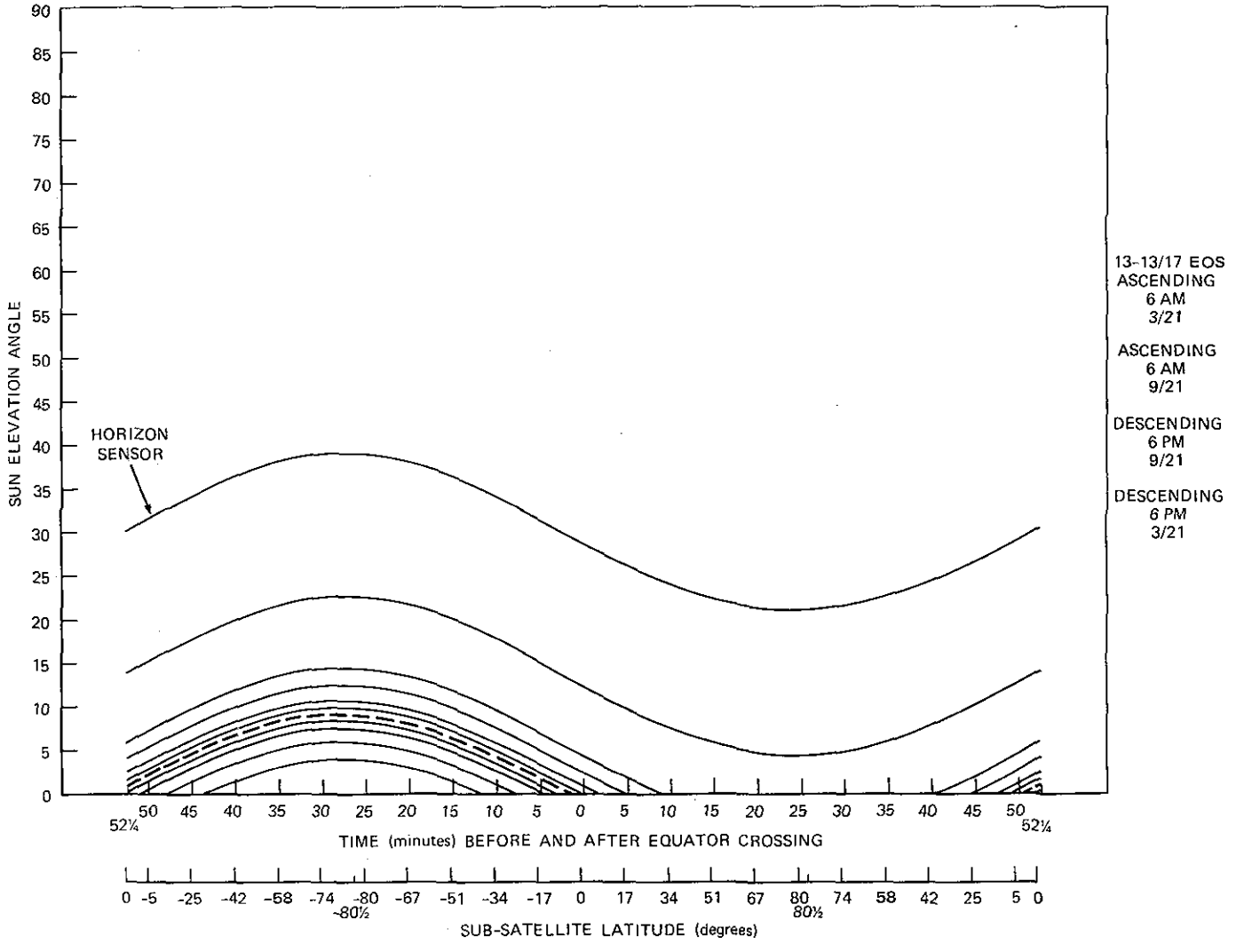

Figure 3. Sensor Illumination - Equinox 6 A.M., 6 P.M.

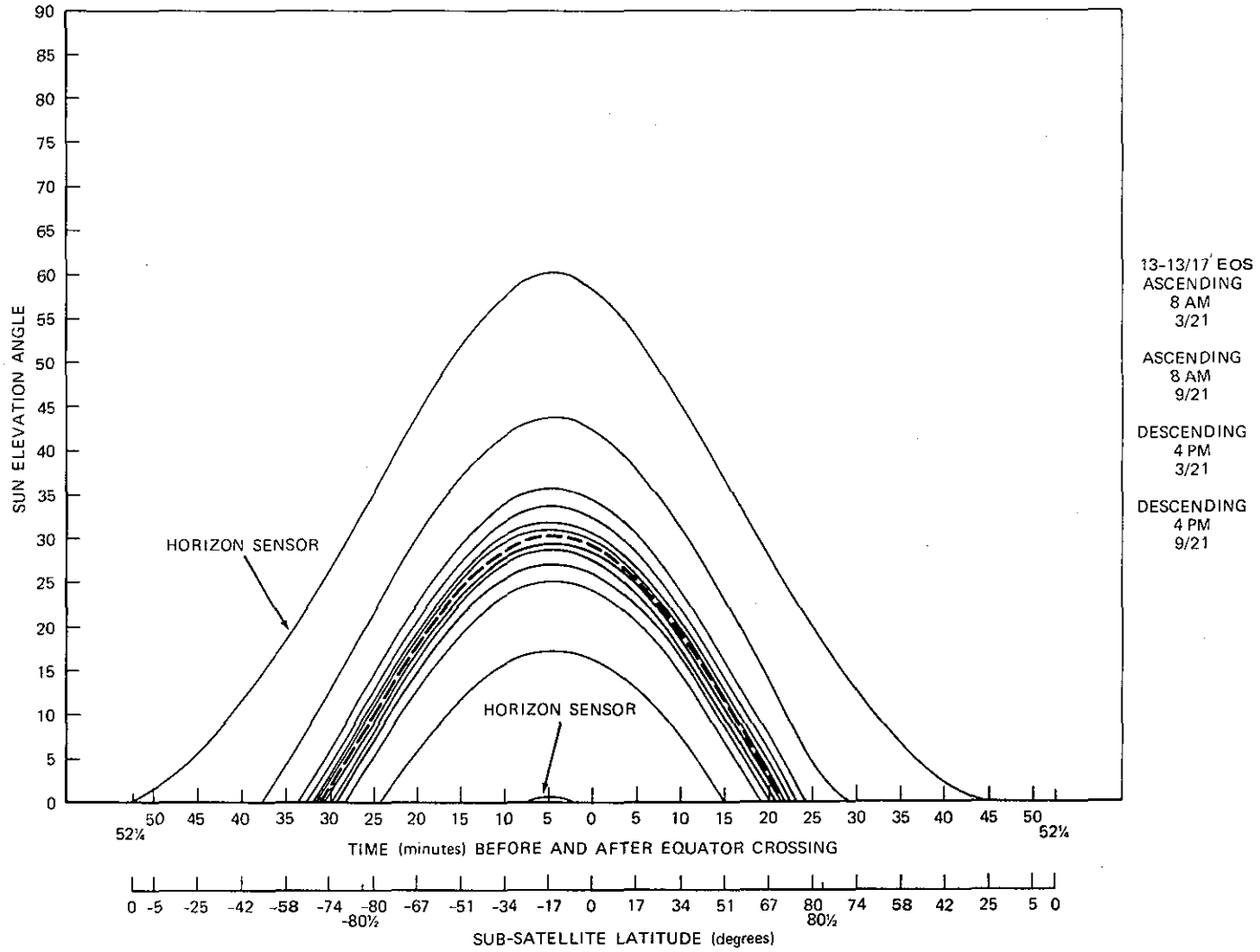

Figure 4. Sensor Illumination - Equinox 8 A.M., 4 P.M.

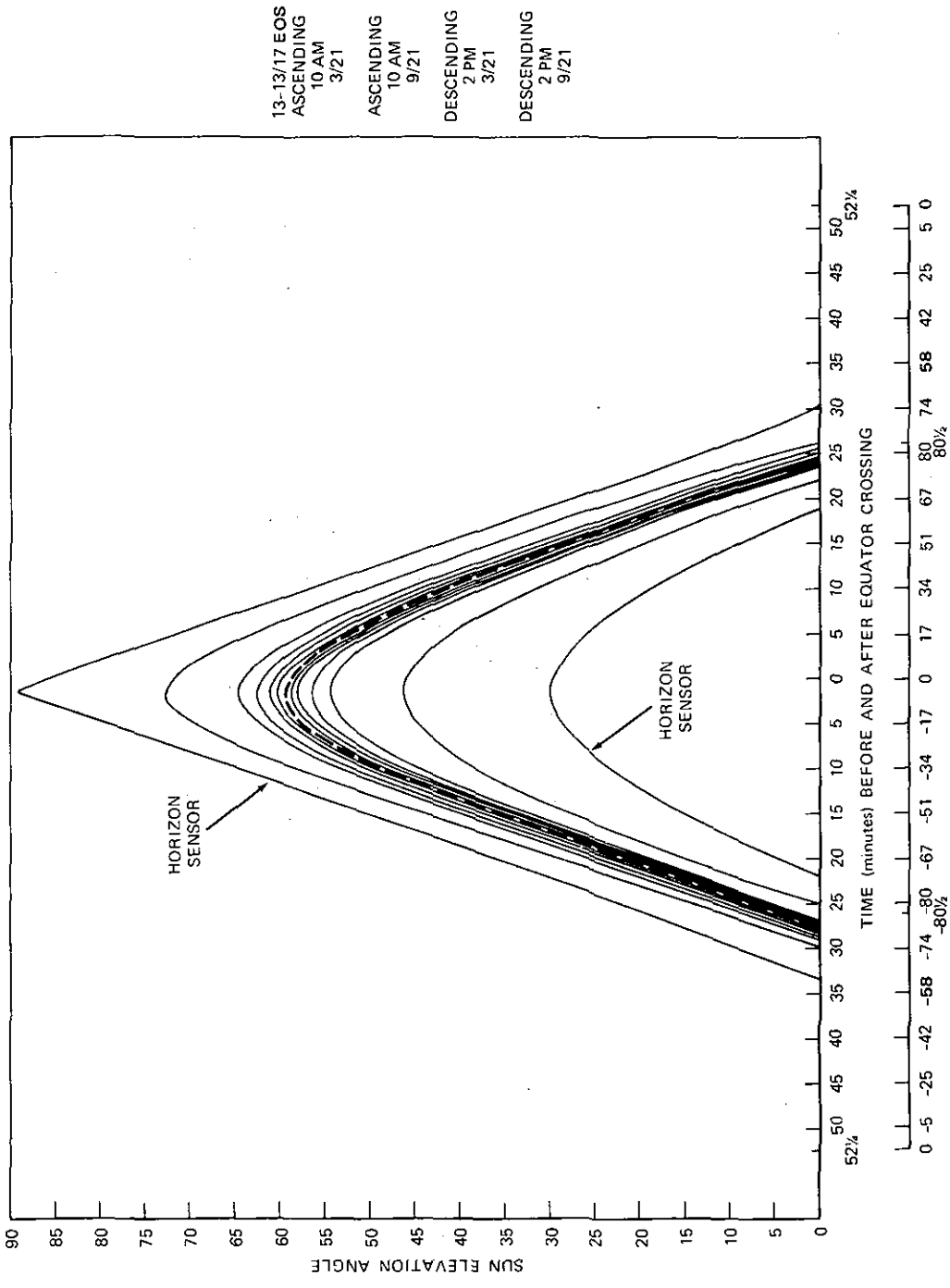

Figure 5. Sensor Illumination - Equinox 10 A.M., 2 P.M.

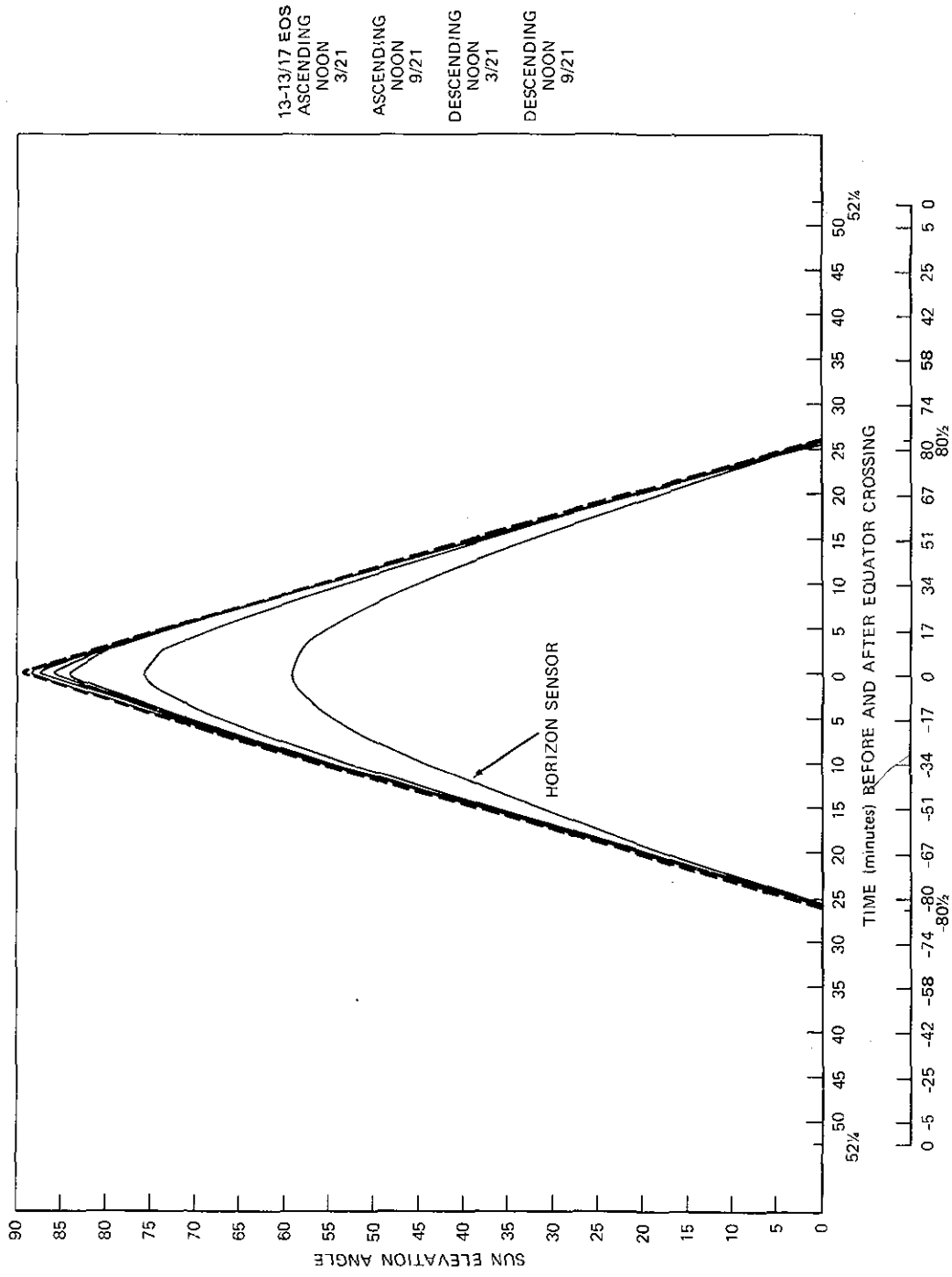

Figure 6. Sensor Illumination - Equinox Noon

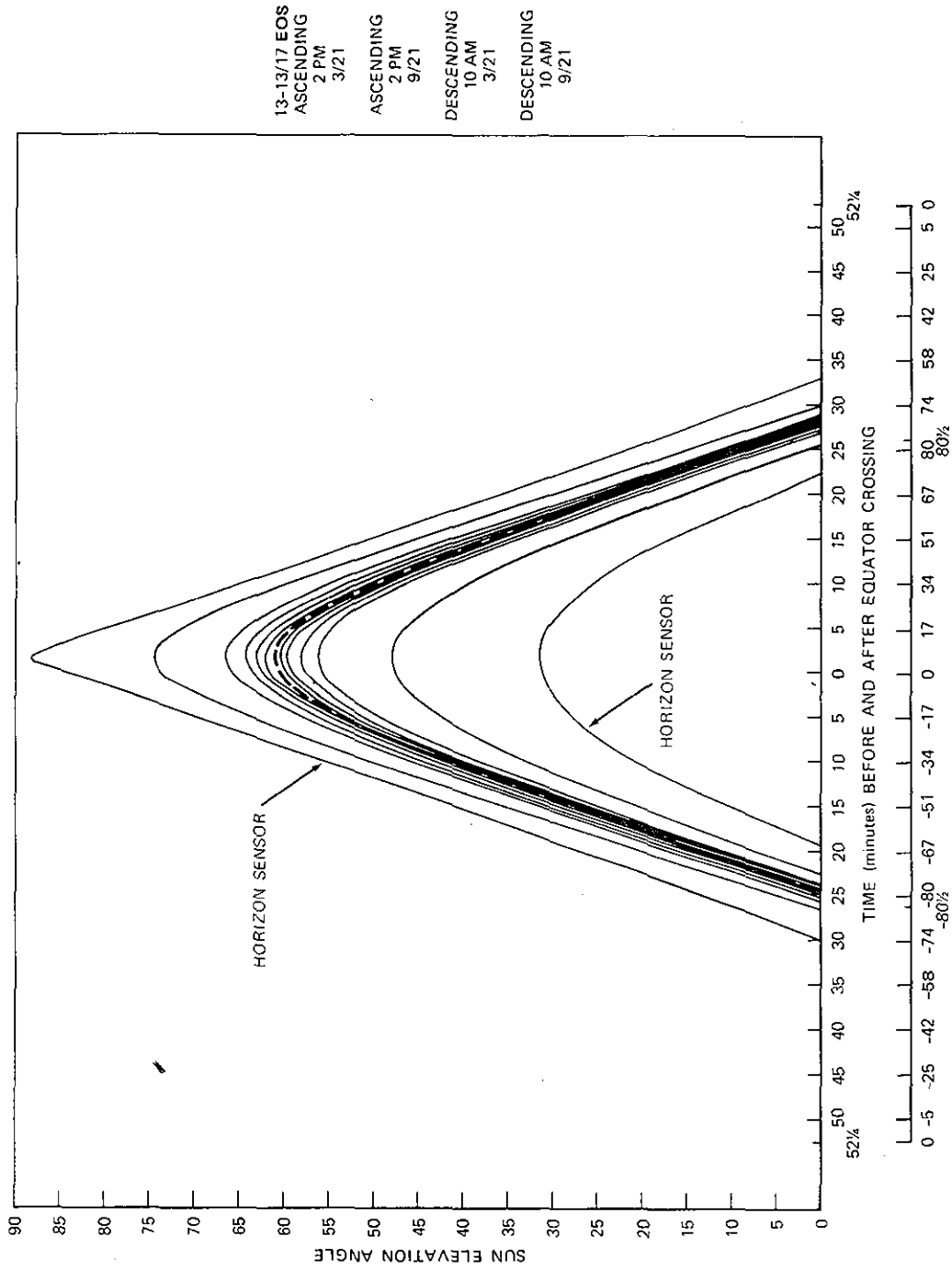

Figure 7. Sensor Illumination - Equinox 2 P.M., 10 A.M.

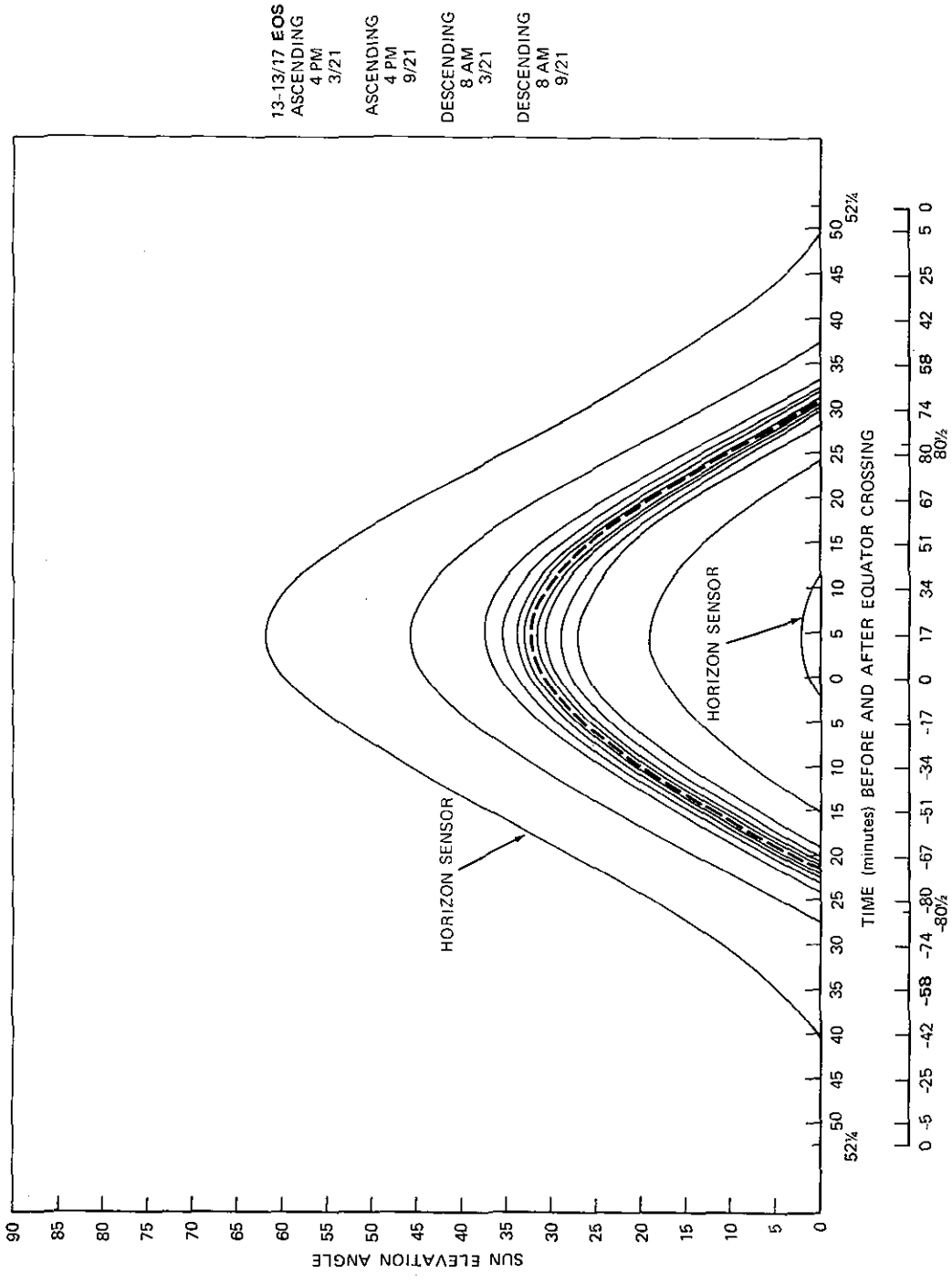

Figure 8. Sensor Illumination - Equinox 4 P.M., 8 A.M.

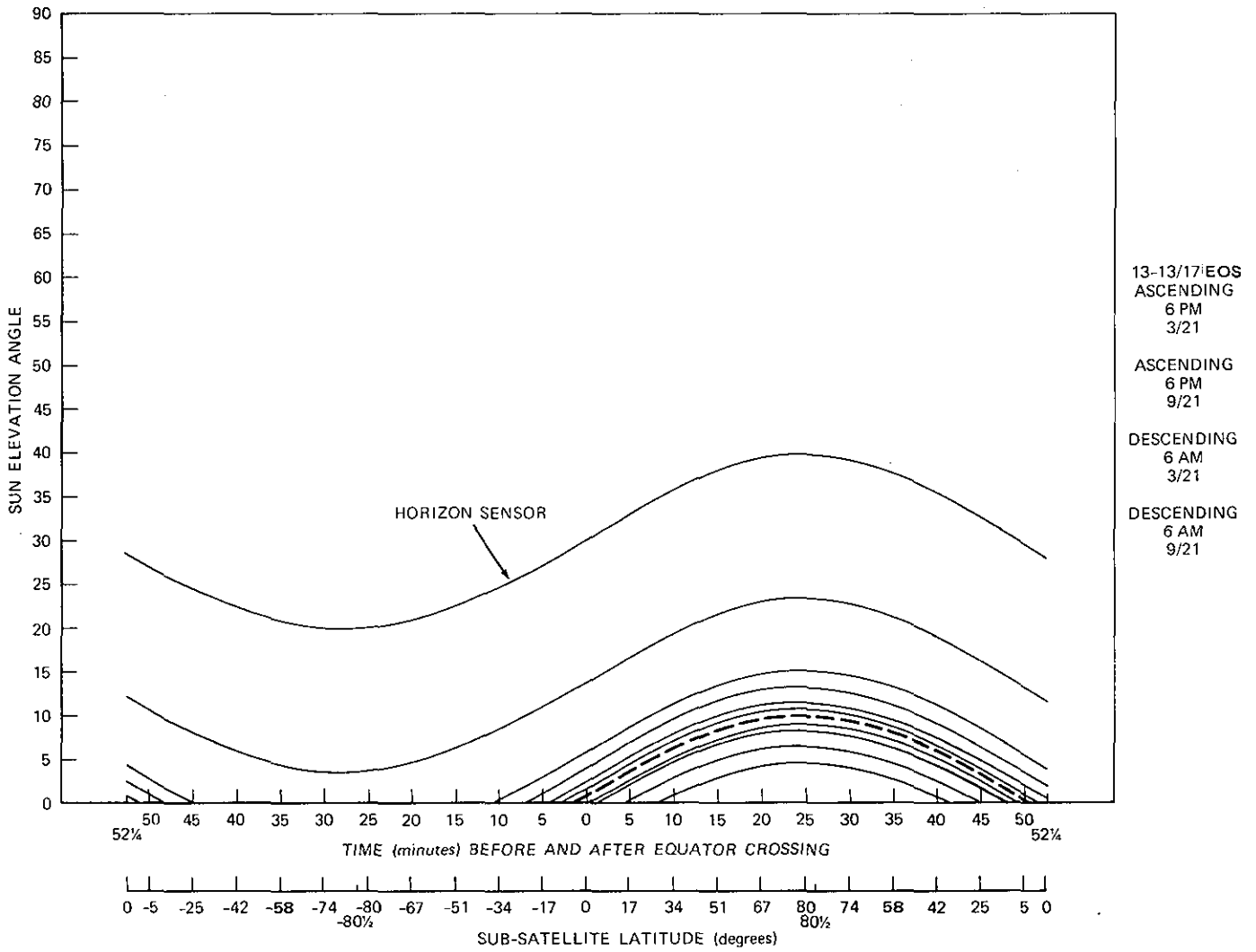

Figure 9. Sensor Illumination – Equinox 6 P.M., 6 A.M.

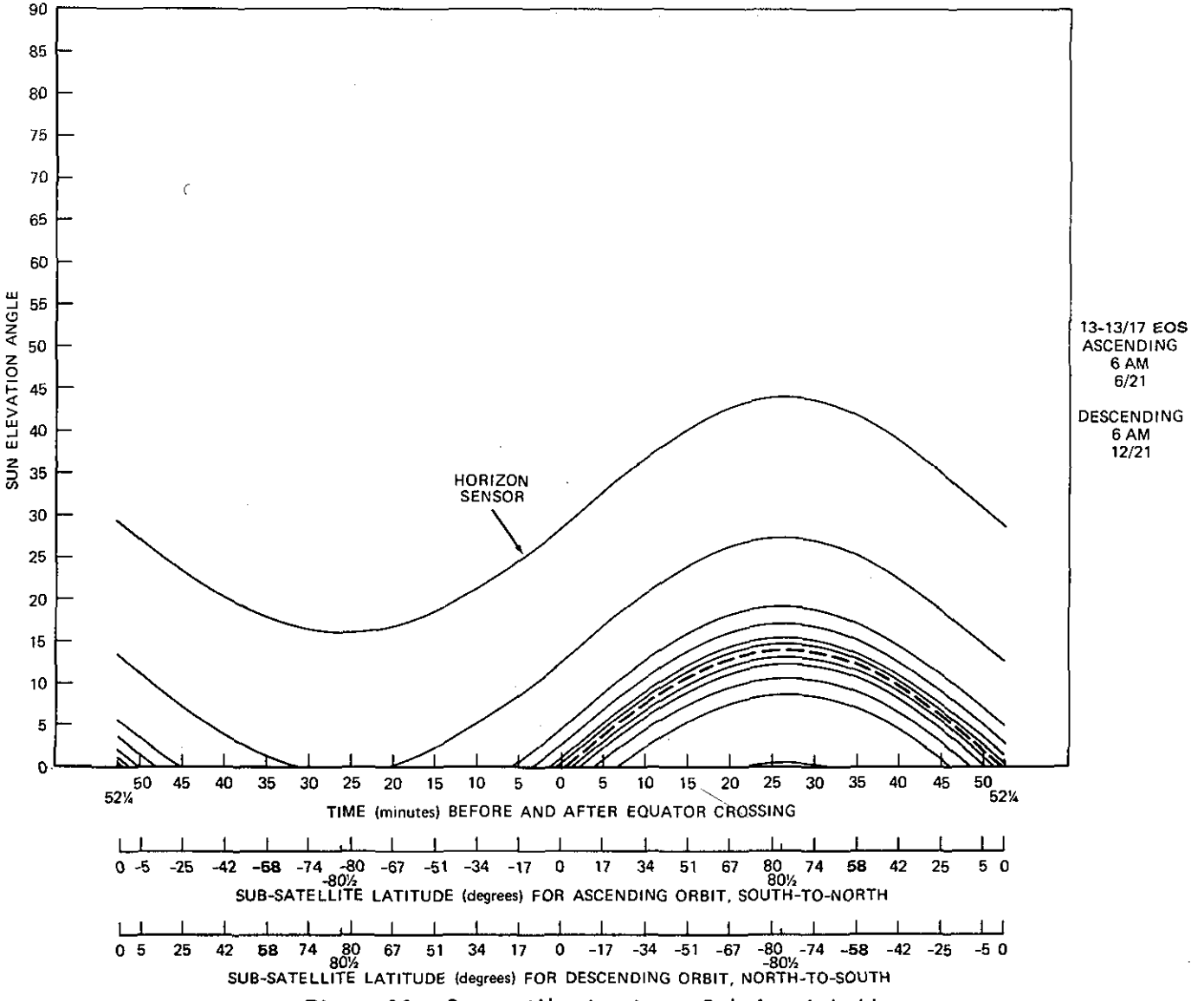

Figure 10. Sensor Illumination - Solstice 6 A.M.

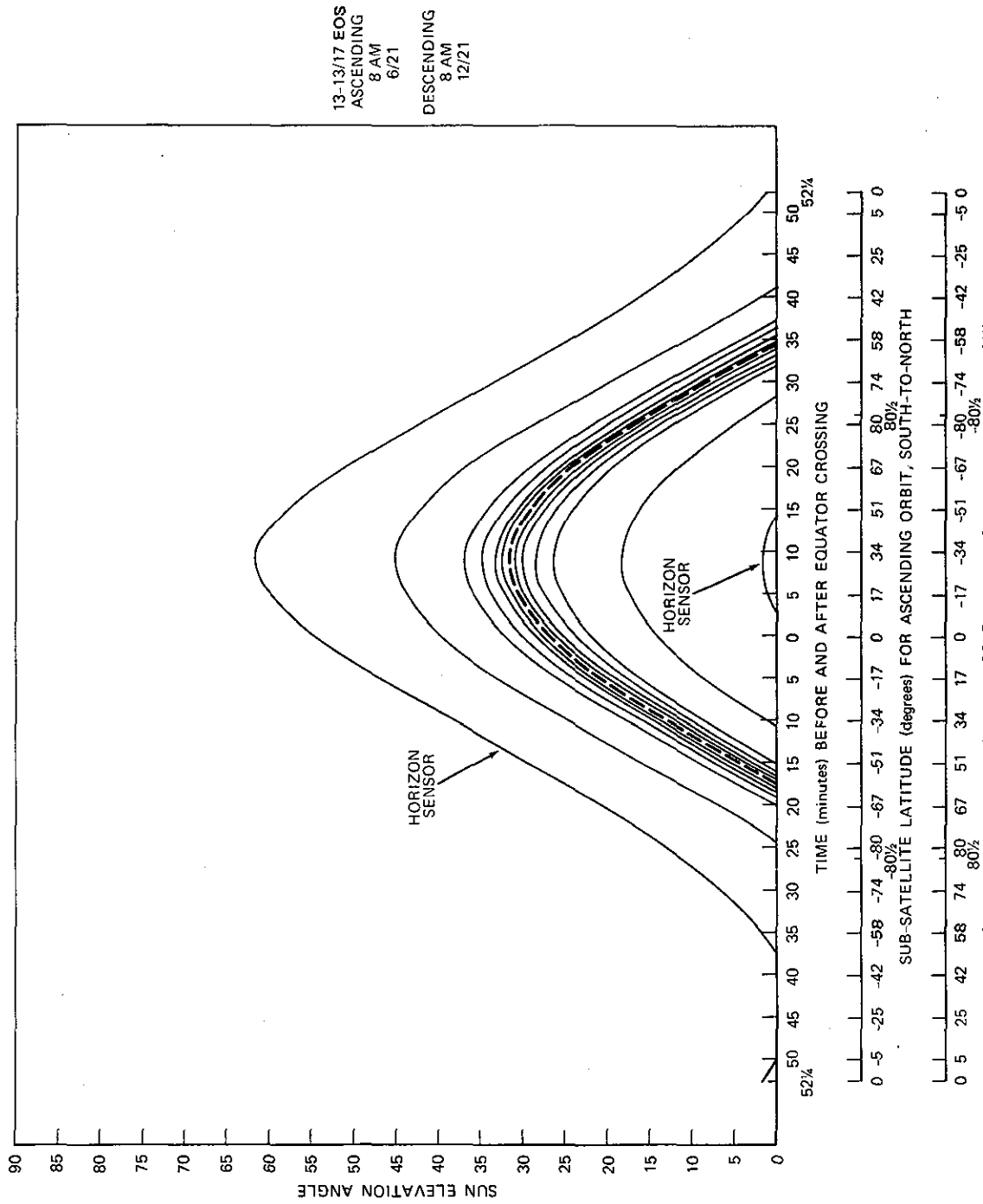

Figure 11. Sensor Illumination – Solstice 8 A.M.

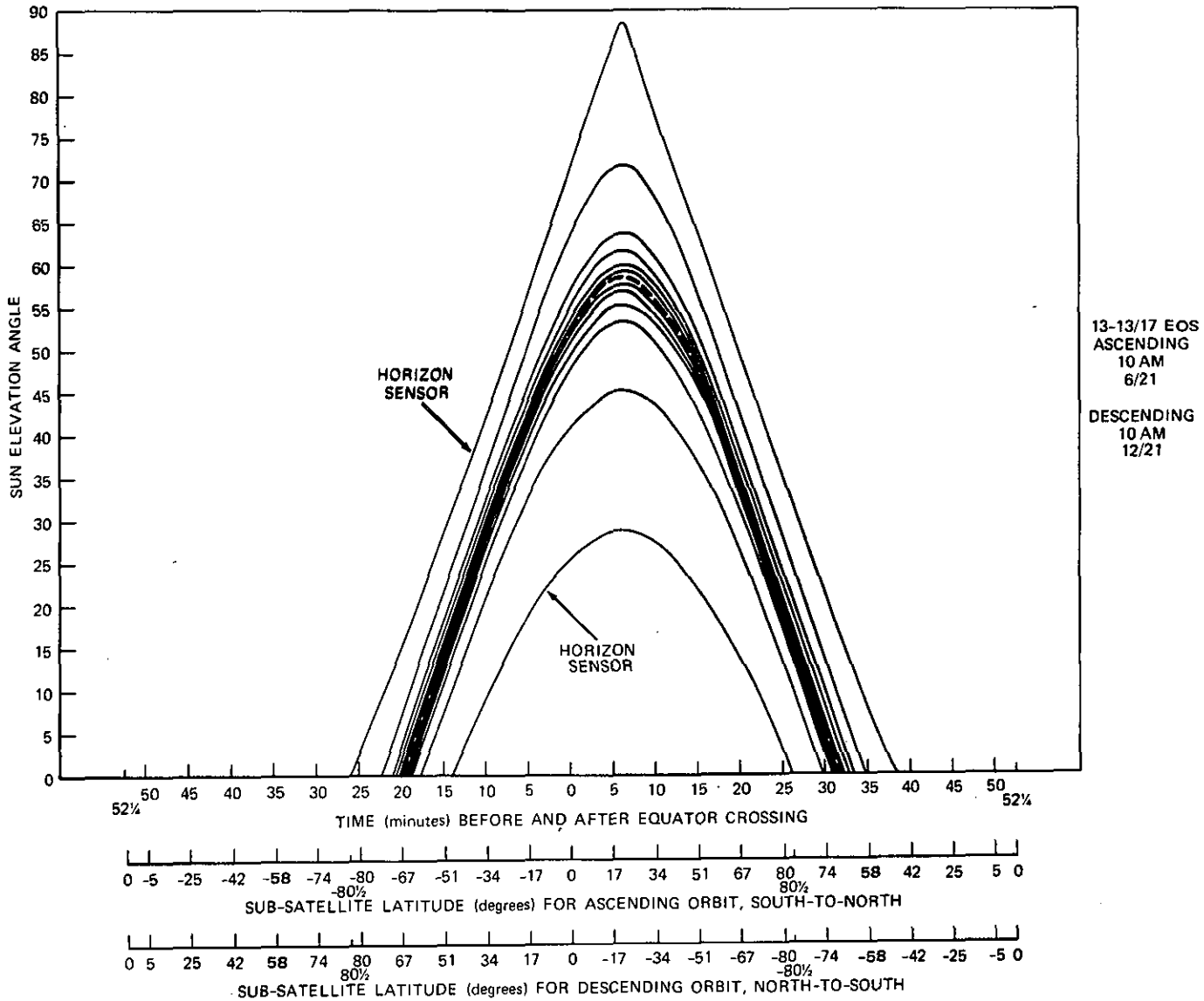

Figure 12. Sensor Illumination - Solstice 10 A.M.

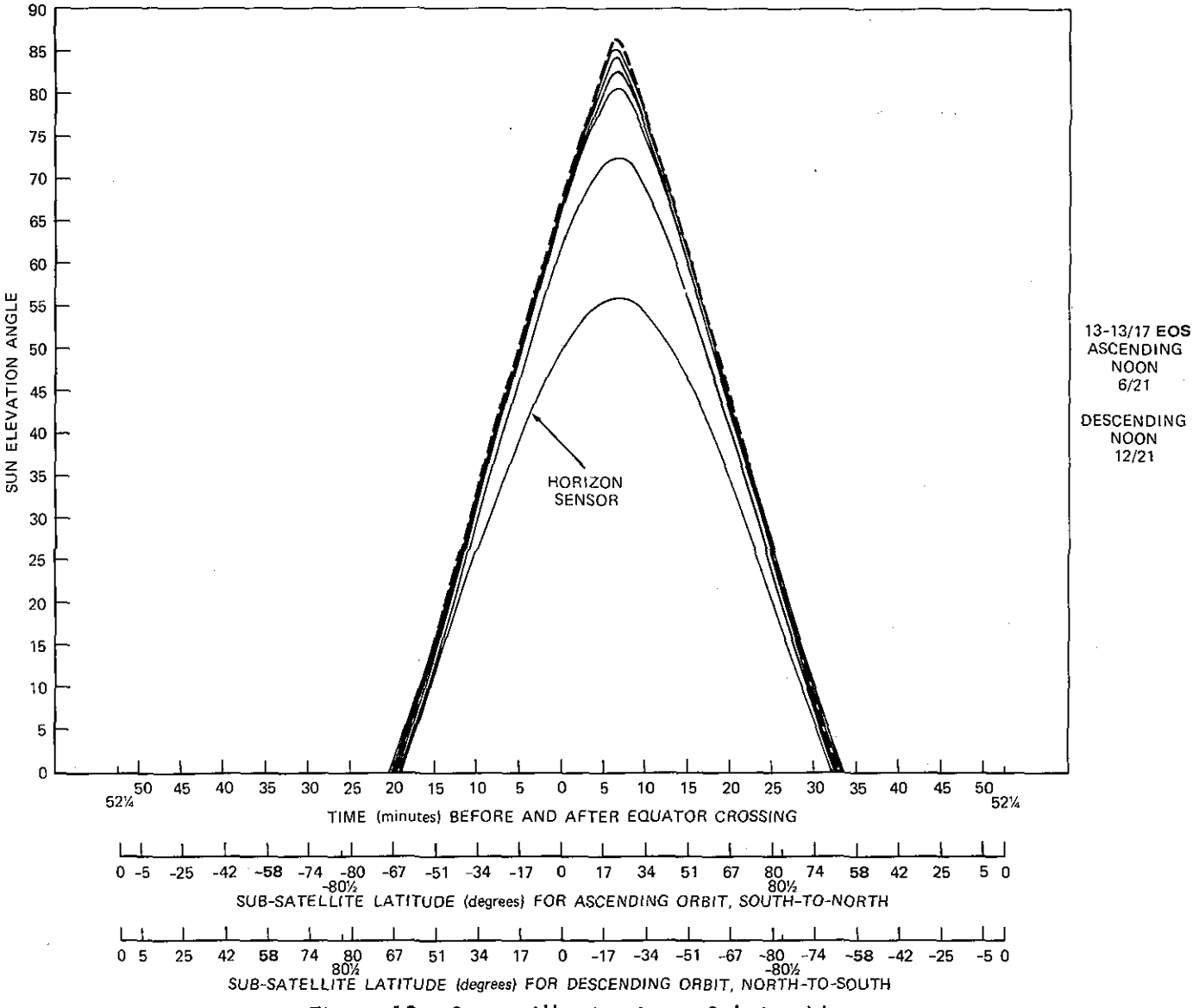

Figure 13. Sensor Illumination - Solstice Noon

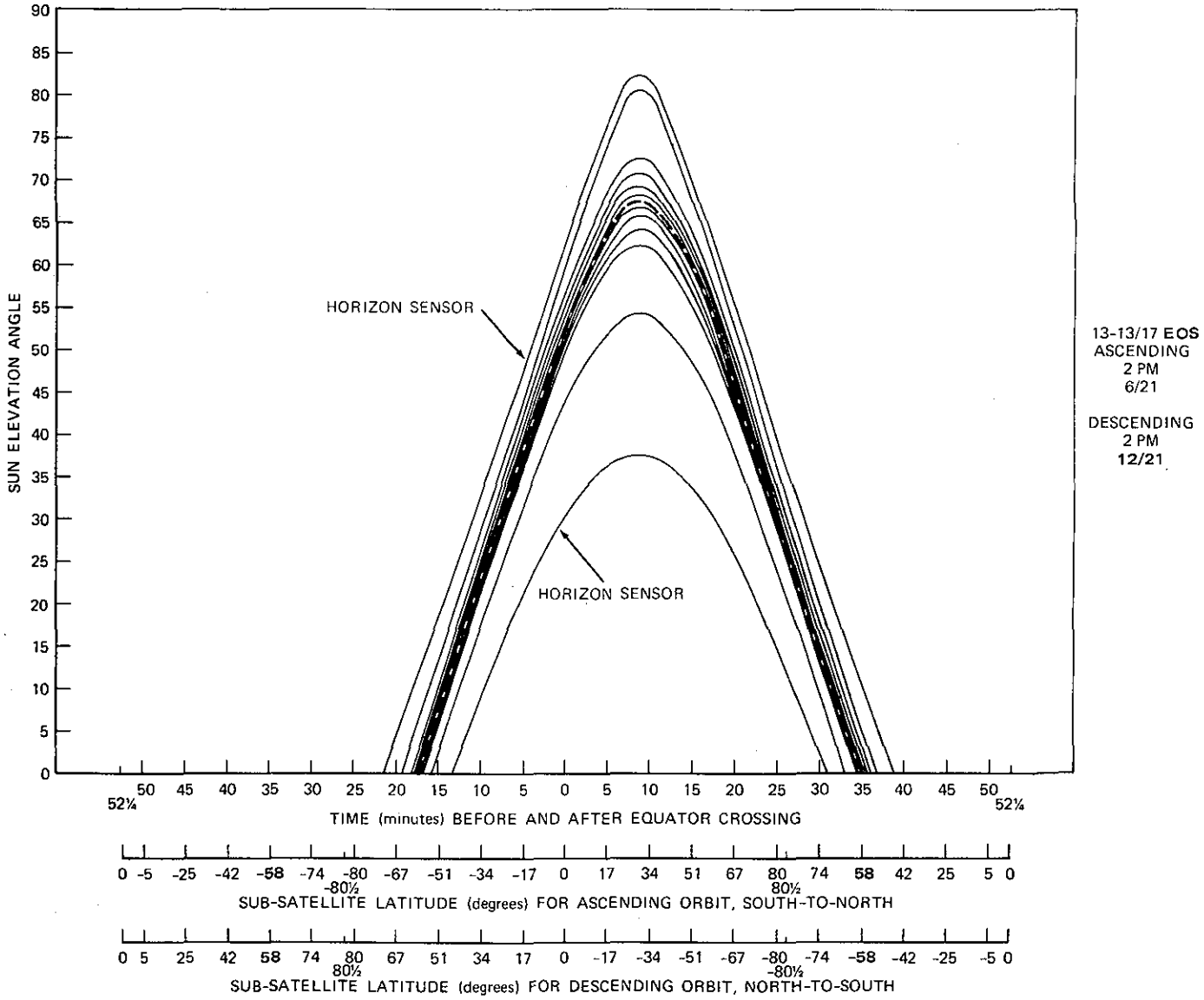

Figure 14. Sensor Illumination - Solstice 2 P.M.

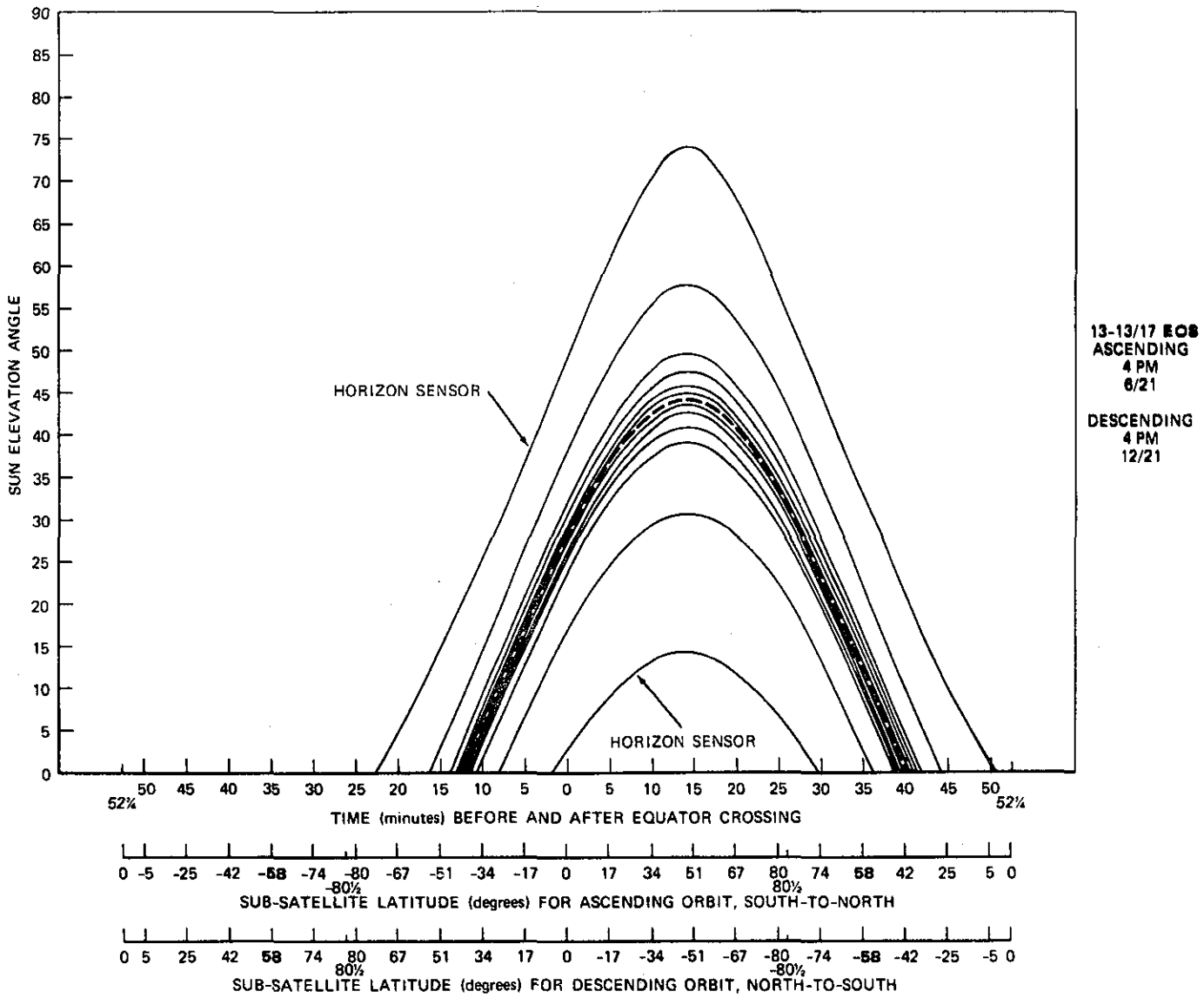

Figure 15. Sensor Illumination - Solstice 4 P.M.

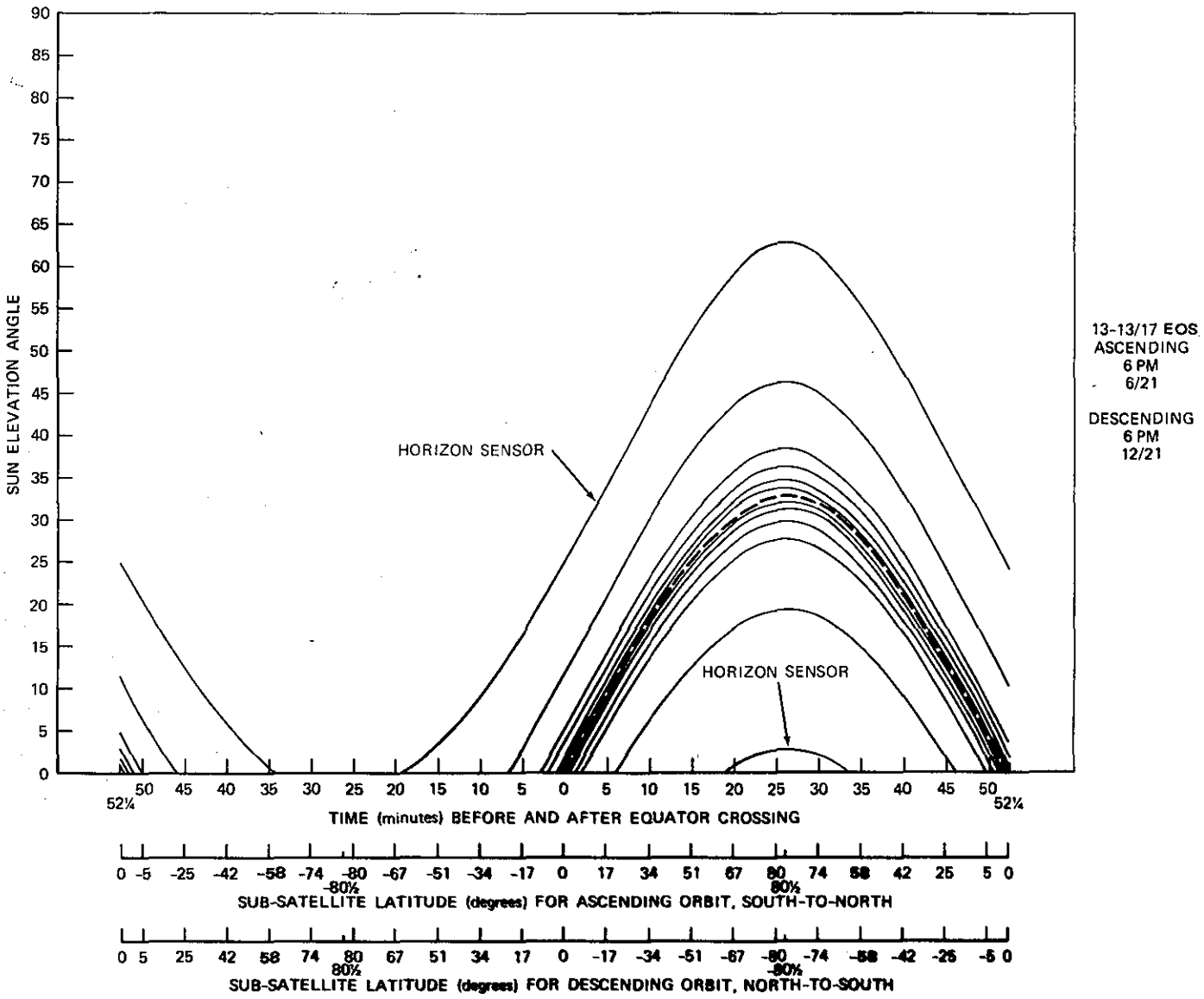

Figure 16. Sensor Illumination – Solstice 6 P.M.

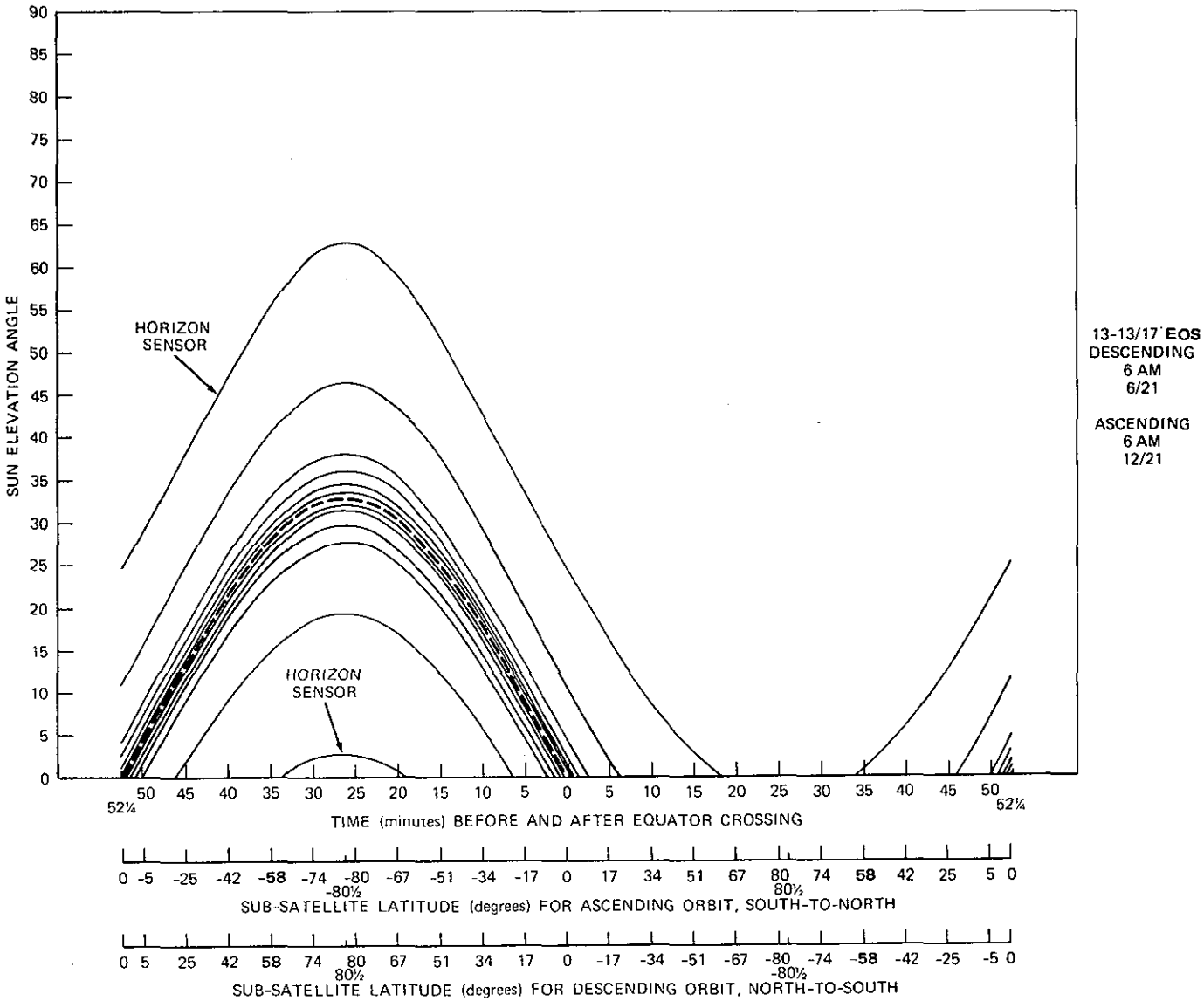

Figure 17. Sensor Illumination - Solstice 6 A.M.

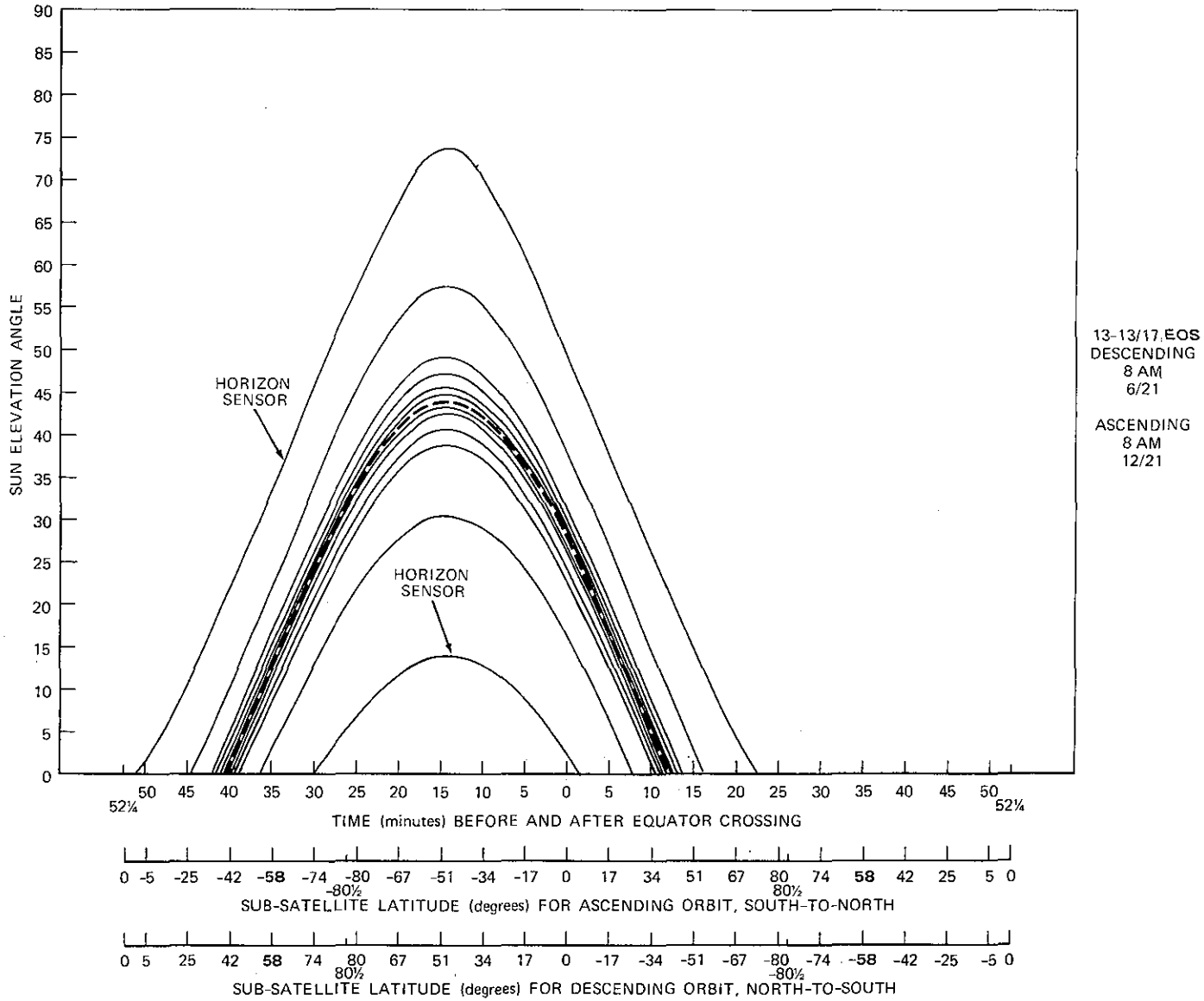

Figure 18. Sensor Illumination - Solstice 8 A.M.

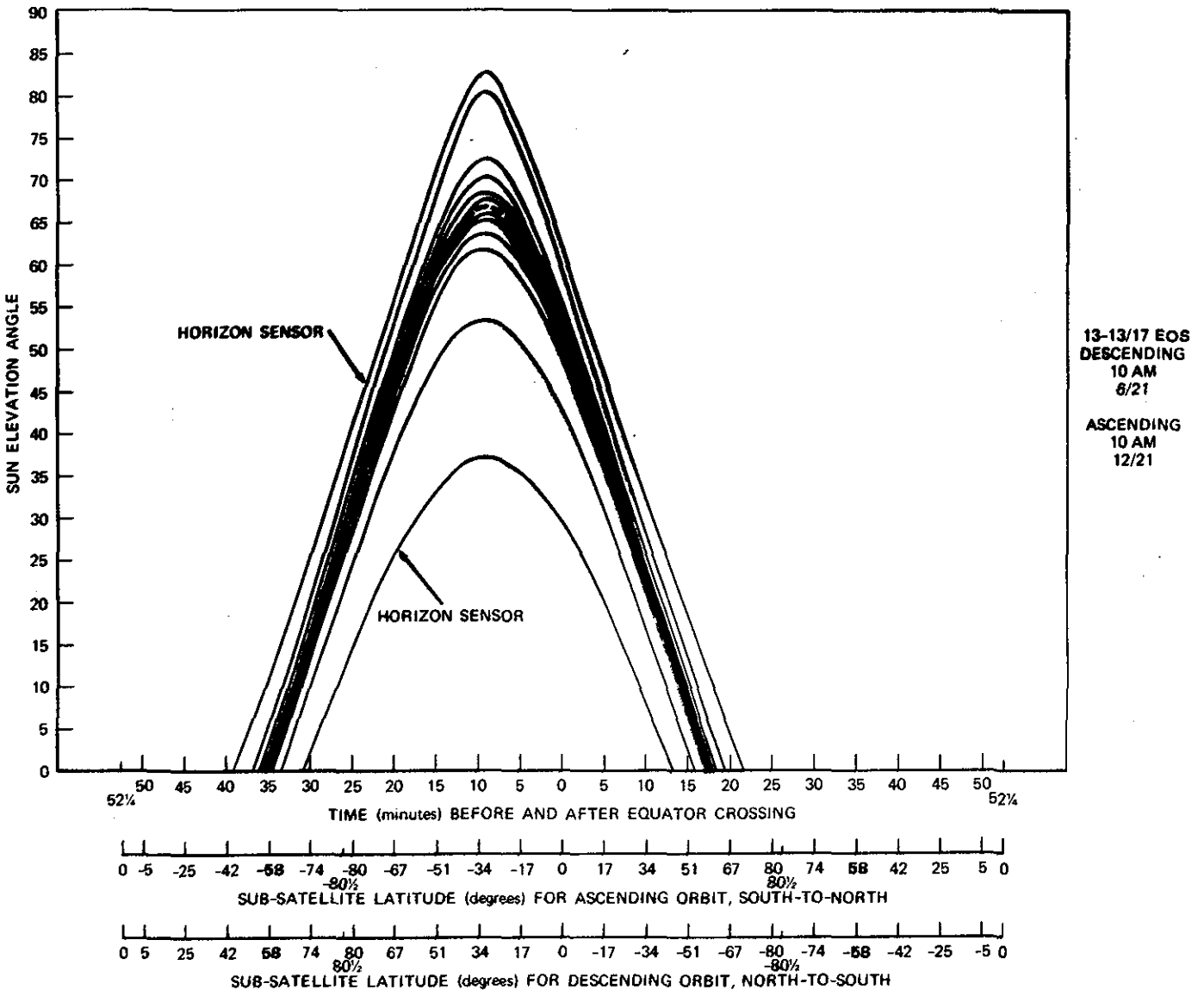

Figure 19. Sensor Illumination - Solstice 10 A.M.

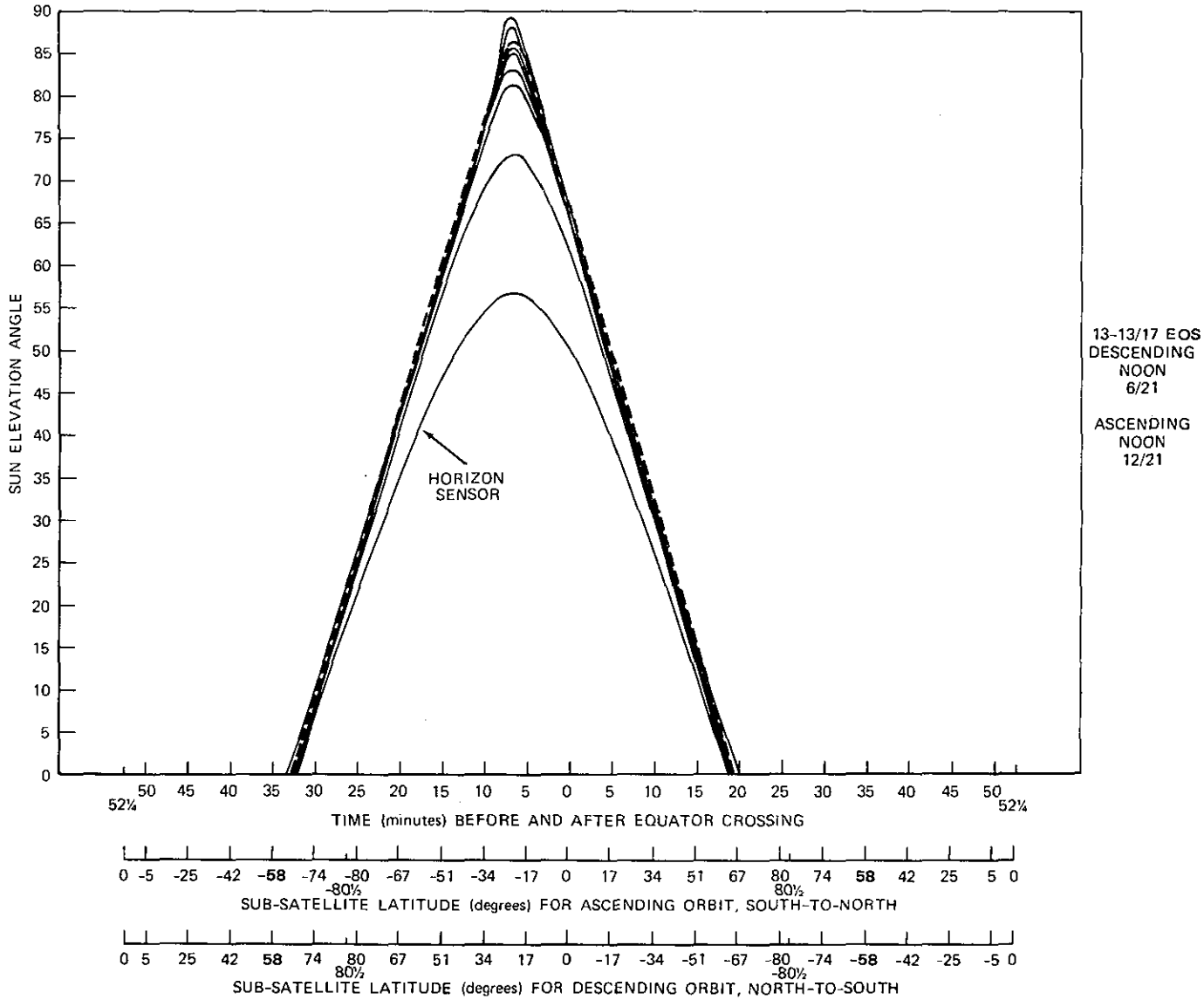

Figure 20. Sensor Illumination - Solstice Noon

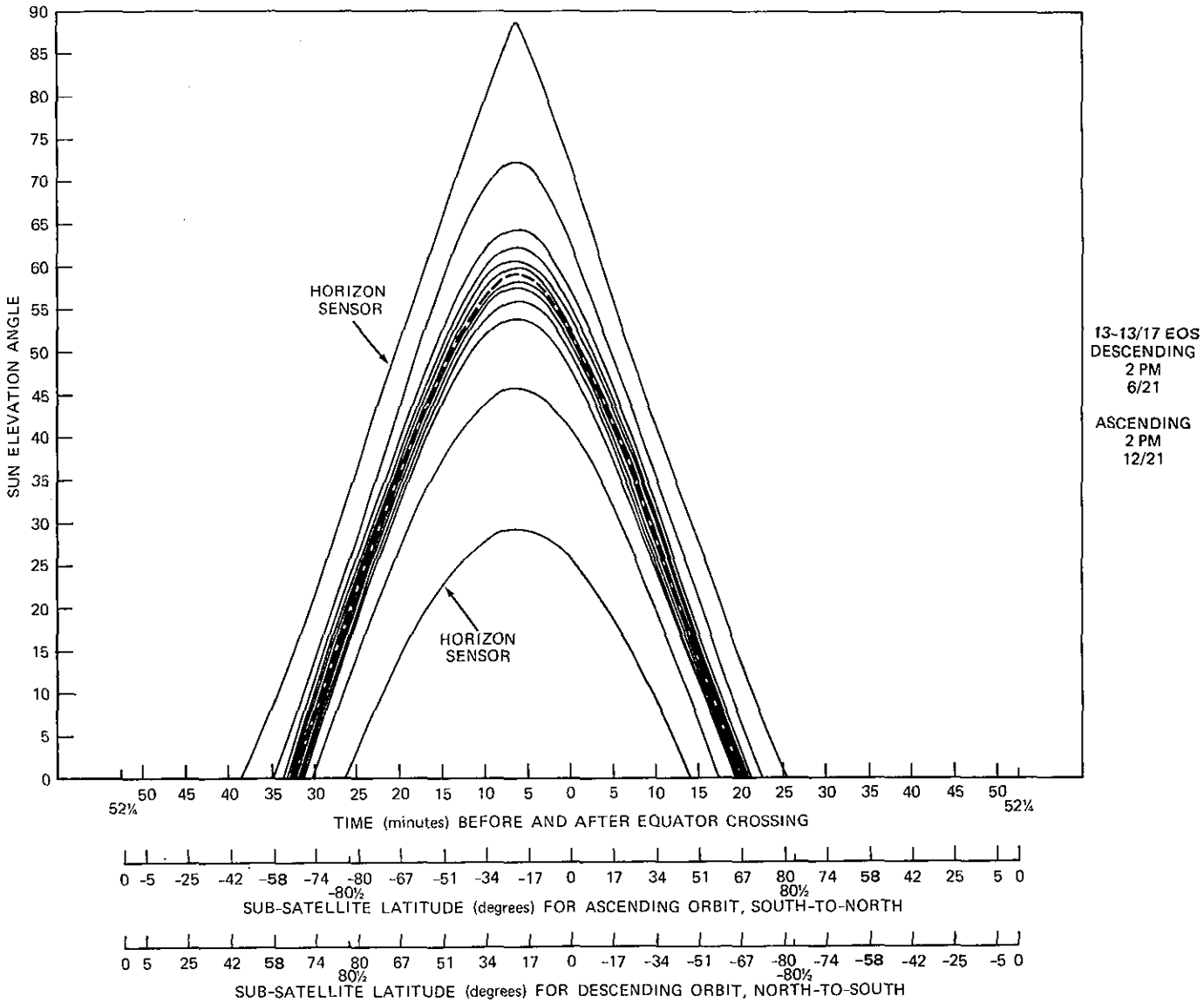

Figure 21. Sensor Illumination - Solstice 2 P.M.

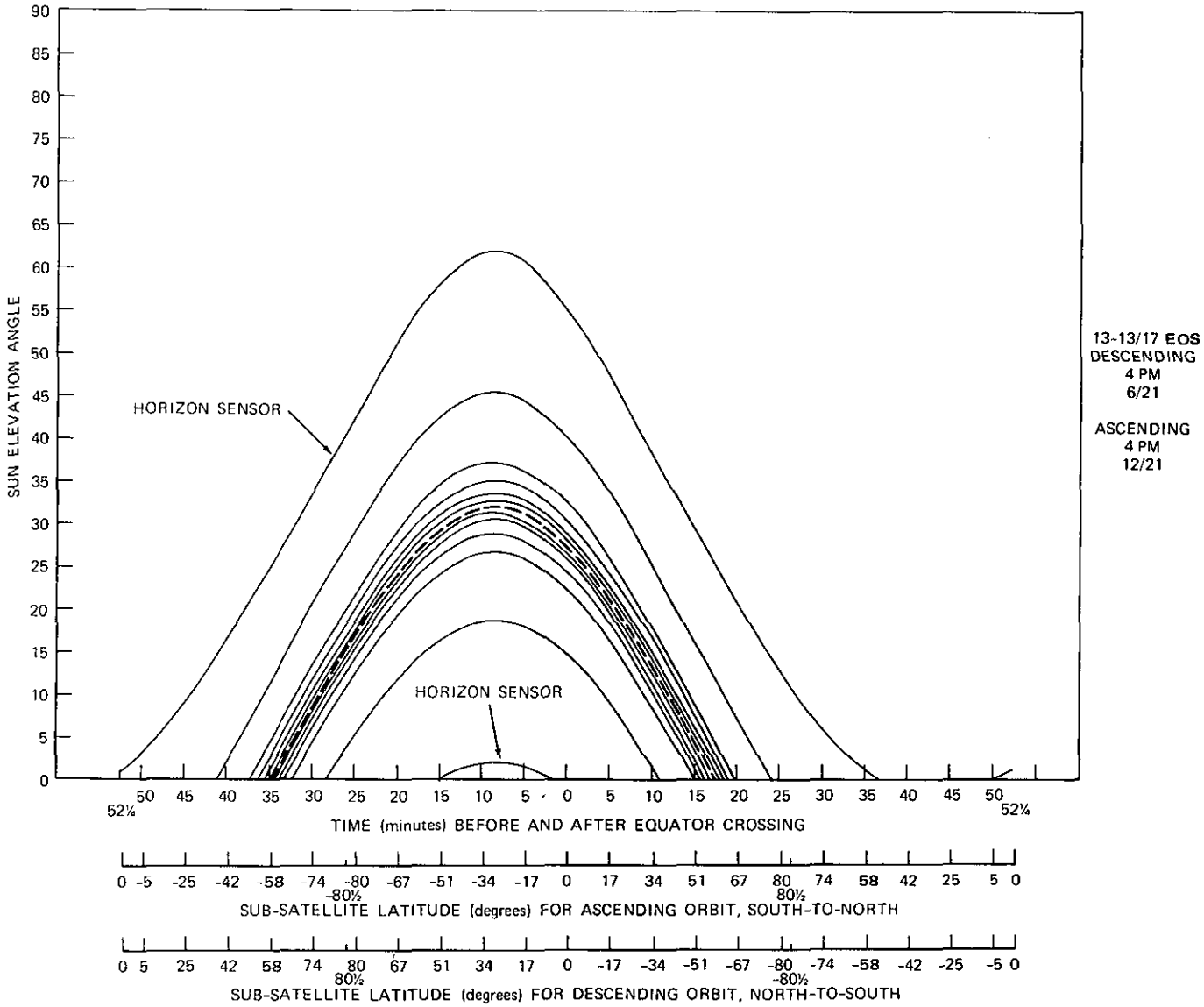

Figure 22. Sensor Illumination - Solstice 4 P.M.

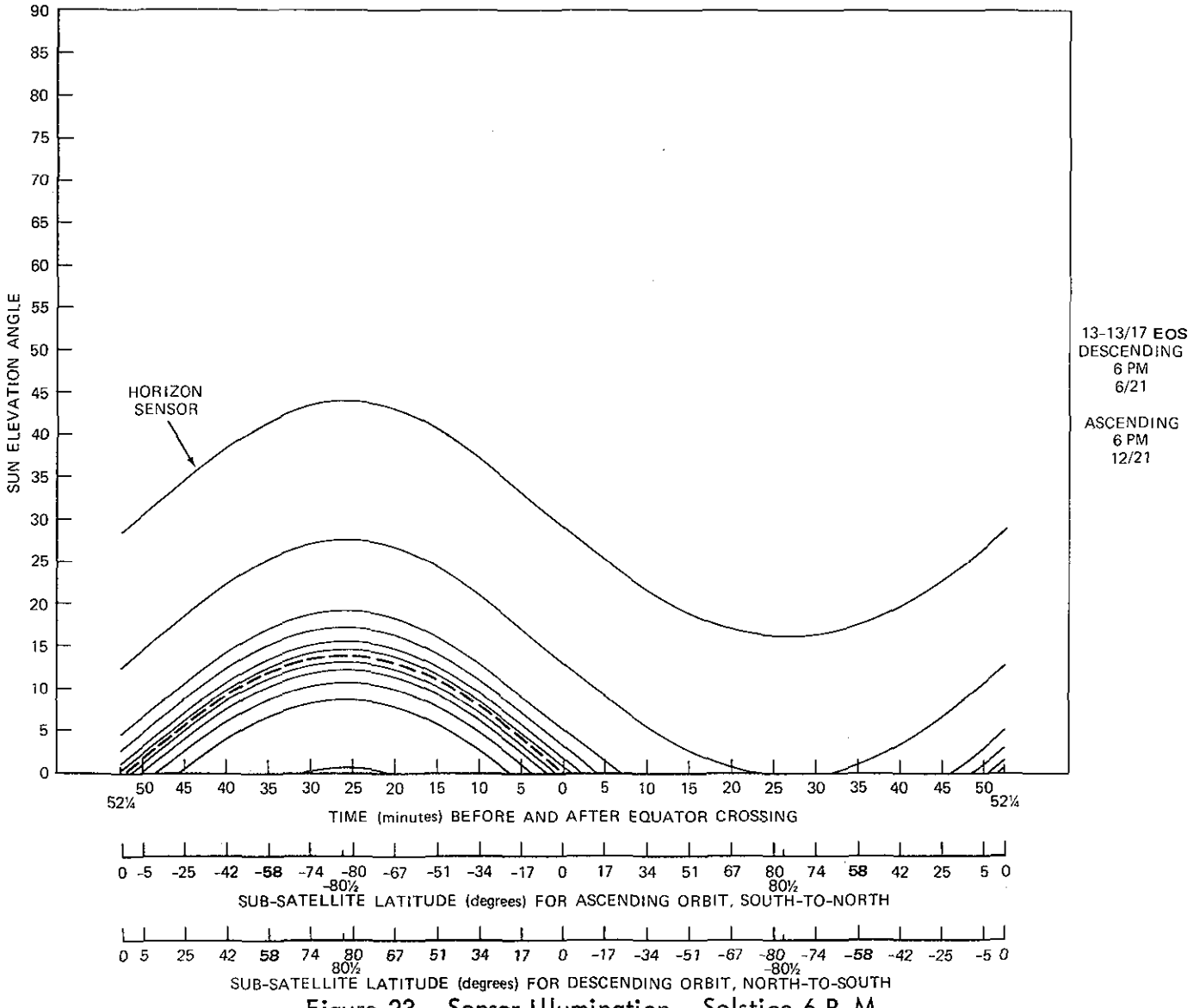

Figure 23. Sensor Illumination - Solstice 6 P.M.

GLINT ANALYSIS

The sun's rays will reflect off the ocean and possibly interfere with usage of the various spacecraft sensors. Assuming a smooth ocean, there is some point such that the sun's rays are reflected exactly at the spacecraft. This point is called the glint point. The goal of this section is to calculate the glint point. The following section will determine the glint points for EOS orbits with various nodes, which means that the sun-spacecraft relative positions are different, and compare with the sensor line coverage.

Consider the sun's rays reflecting off the smooth surface:

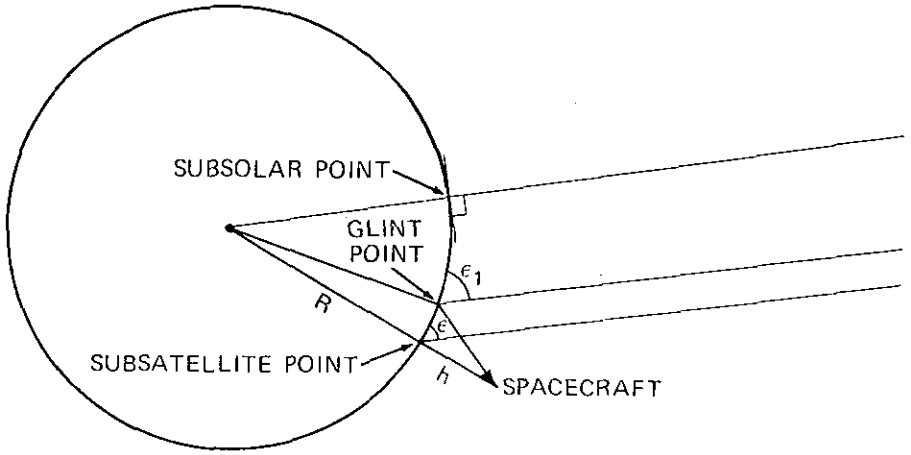

The latitude and longitude of the subsolar point may be found. At this point the sun-earth vector pierces the earth, and because the sun is directly overhead at this point the solar elevation angle is 90 degrees. A second reference point is the subsatellite point. Let the solar elevation angle at this point be ϵ. Consider the great circle on the surface of the earth connecting the subsolar point and the subsatellite point. To have a ray of the sun be reflected into the spacecraft means that the glint point must be on this great circle. Consider also the variation in sun elevation angle along this great circle. The sun elevation angle varies from 90 degrees at the subsolar point to ϵ at the subsatellite point. To find the intermediate sun elevation angle ϵ_1, consider the triangle:

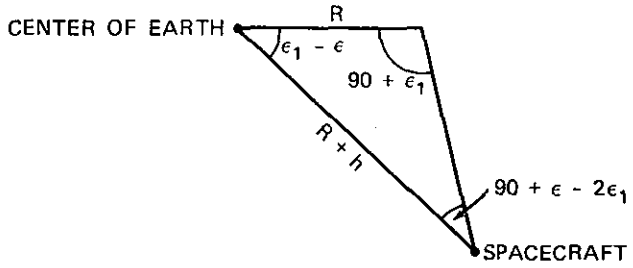

Then,

$$\frac{R}{\sin (90 + \epsilon - 2\epsilon_1)} = \frac{R + h}{\sin (90 + \epsilon_1)}$$

or

$$\frac{R + h}{R} = \frac{\sin (90 + \epsilon_1)}{\sin (90 + \epsilon - 2\epsilon_1)} = \frac{\cos \epsilon_1}{\cos (2\epsilon_1 - \epsilon)}.$$

Since R, h, and ϵ are known, an iteration procedure will find ϵ_1 such that:

$$\frac{R + h}{R} = \frac{\cos \epsilon_1}{\cos (2\epsilon_1 - \epsilon)}.$$

Once ϵ_1 is known, considering that the sun elevation angle varies continuously along the great circle between a value of 90 degrees at the subsolar point and ϵ at the subsatellite point, an iteration procedure will then give the latitude and longitude of the glint point.

Glint Points and Glint Trace Pattern

The glint point at a given time is determined by the relationship between the sun's position and the spacecraft position. In Figure 24 an ascending 10 A.M. orbit near the vernal equinox is taken. Thus the sun is approximately 30 degrees east of the orbit at the equator crossing. The approximate glint point at 2 minute intervals is given by an "x". The glint points are toward the sun, but nearer the subsatellite point than the subsolar point. The figure also shows the motion of the sun in the time period. The sensor coverage is assumed perpendicular to the orbital ground trace — thus an important question is when and where the glint point is on the line for sensor coverage. This could occur in three places on the orbit; (1) near the descending node, which in this case is in darkness, (2) when the subsatellite point is near 75 degrees north, also in darkness in this case, and (3) most importantly near the ascending node. When the subsatellite point is nearly 5 degrees south latitude, a line perpendicular to the orbit passes through the glint point. This is denoted on Figure 24 by an arrow, and is thus the place in the orbit where a line sensor viewing perpendicular to the orbit could be rendered ineffective.

Figure 25 gives the ground trace for the glint points for 6 A.M., 8 A.M., 10 A.M., 2 P.M., 4 P.M., and 6 P.M. ascending node equinox orbits. The ground trace of the glint points for a noon orbit is nearly on the subsatellite ground trace, and is thus not shown here. The glint ground trace is given for

that portion of the subsatellite ground track between 70 degrees south latitude and 70 degrees north latitude. Near the equator the glint point for an orbit 2 hours away from noon (10 A.M. or 2 P.M.) occurs about 5 degrees away from the ground track, for an orbit 4 hours away from noon (8 A.M. or 4 P.M.) occurs about 10 degrees away from the ground track, and for an orbit 6 hours away from noon (6 A.M. or 6 P.M.) occurs about 18 degrees away from the ground track. A comparison may then be made with Figure 1, which shows that the ends of the 30 degree width sensor extend about 5 degrees from the ground track and the ends of the 52 degree sensor extend about 13 degrees from the ground track. This comparison of Figures 1 and 25 will then give an indication of the effect of glint on sensors of various widths for different nodes. Another important consideration is the point at which a line perpendicular to the ground track passes through the glint point (i.e., is part of the great circle connecting the subsolar point and the subsatellite point). This occurs at approximately 15 degrees south latitude for the 6 A.M. orbit, 10 degrees south latitude for the 8 A.M. orbit, 5 degrees south latitude for the 10 A.M. orbit, 5 degrees north latitude for the 2 P.M. orbit, 10 degrees north latitude for the 4 P.M. orbit, and 15 degrees north latitude for the 6 P.M. orbit. These are the critical places in the orbit where a sensor could look directly at the glint point.

Figure 26 gives the ground trace for the glint points for the summer solstice, when the subsolar point has approximately 23-1/2 degree north latitude. Figure 27 gives the ground trace for the glint points for the winter solstice, when the subsolar point has approximately 23-1/2 degree south latitude. The points along the orbit at which a line perpendicular to the ground track passes through the glint point are also given. Three further cases, similar to Figures 25-27, for the descending node equinox orbits, and ascending nodes summer and winter solstice will be referred to but not presented in figures. Referring to Figure 25 it is noticed that the points along the orbit for the ascending node cases occur at latitudes 5°, 10°, and 15° above and below the subsolar latitude; this also holds for other subsolar latitudes from 23-1/2 degrees south to 23-1/2 degrees north. Referring to Figures 26 and 27 this is seen to be true for the descending node cases where the subsolar latitude is 23-1/2 degrees north (summer solstice) and 23-1/2 degrees south (winter solstice). Thus a table can be generated which shows the latitudes of points along the orbit during the course of a year whereby a line perpendicular to the ground track passes through the glint point.

Orbit	Range of Subsatellite Latitudes whereby a Line Sensor Looks Directly at a Glint Point Sometime During the Year
Ascending Node 6 A.M.	38-1/2° S to 8-1/2° N
Ascending Node 8 A.M.	33-1/2° S to 13-1/2° N
Ascending Node 10 A.M.	28-1/2° S to 18-1/2° N
Ascending Node 2 P.M.	18-1/2° S to 28-1/2° N
Ascending Node 4 P.M.	13-1/2° S to 33-1/2° N
Ascending Node 6 P.M.	8-1/2° S to 38-1/2° N
Descending Node 6 A.M.	8-1/2° S to 38-1/2° N
Descending Node 8 A.M.	13-1/2° S to 33-1/2° N
Descending Node 10 A.M.	18-1/2° S to 28-1/2° N
Descending Node 2 P.M.	28-1/2° S to 18-1/2° N
Descending Node 4 P.M.	33-1/2° S to 13-1/2° N
Descending Node 6 P.M.	38-1/2° S to 8-1/2° N

This then gives that part of the orbit affected by a glint problem sometime during the course of a year.

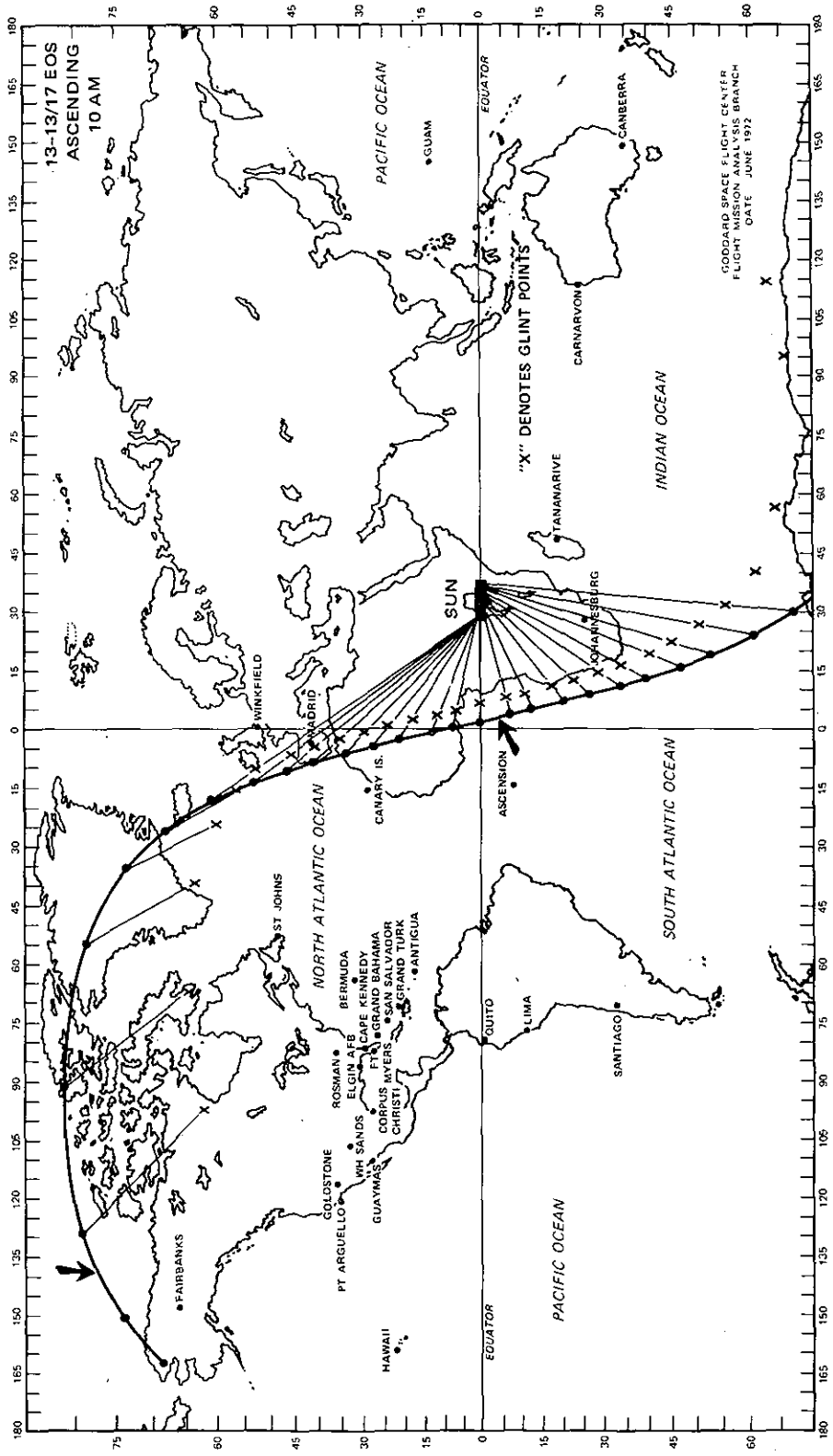

Figure 24. Glint Points

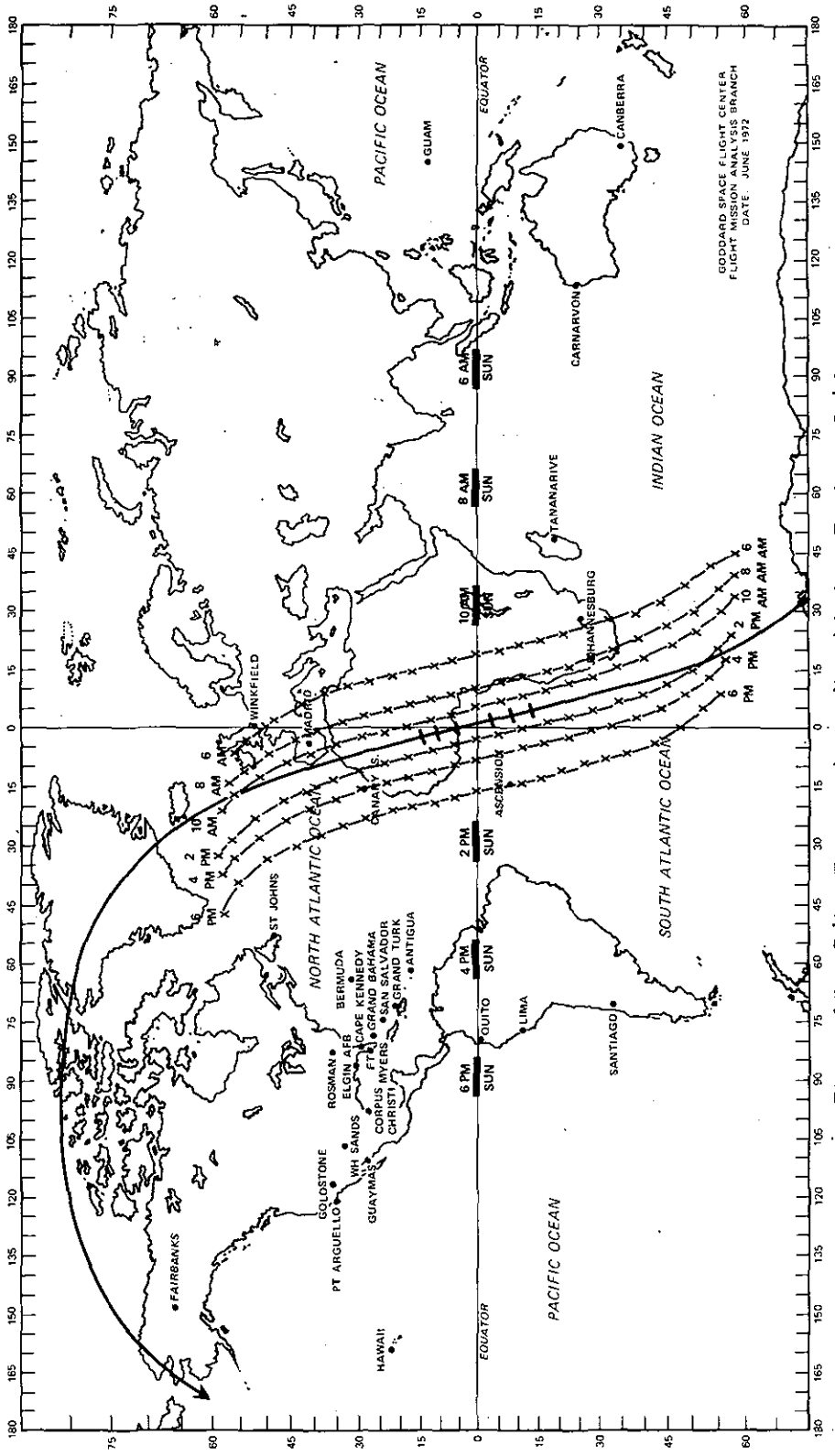

Figure 25. Glint Trace – Ascending Nodes, Equinox Orbits

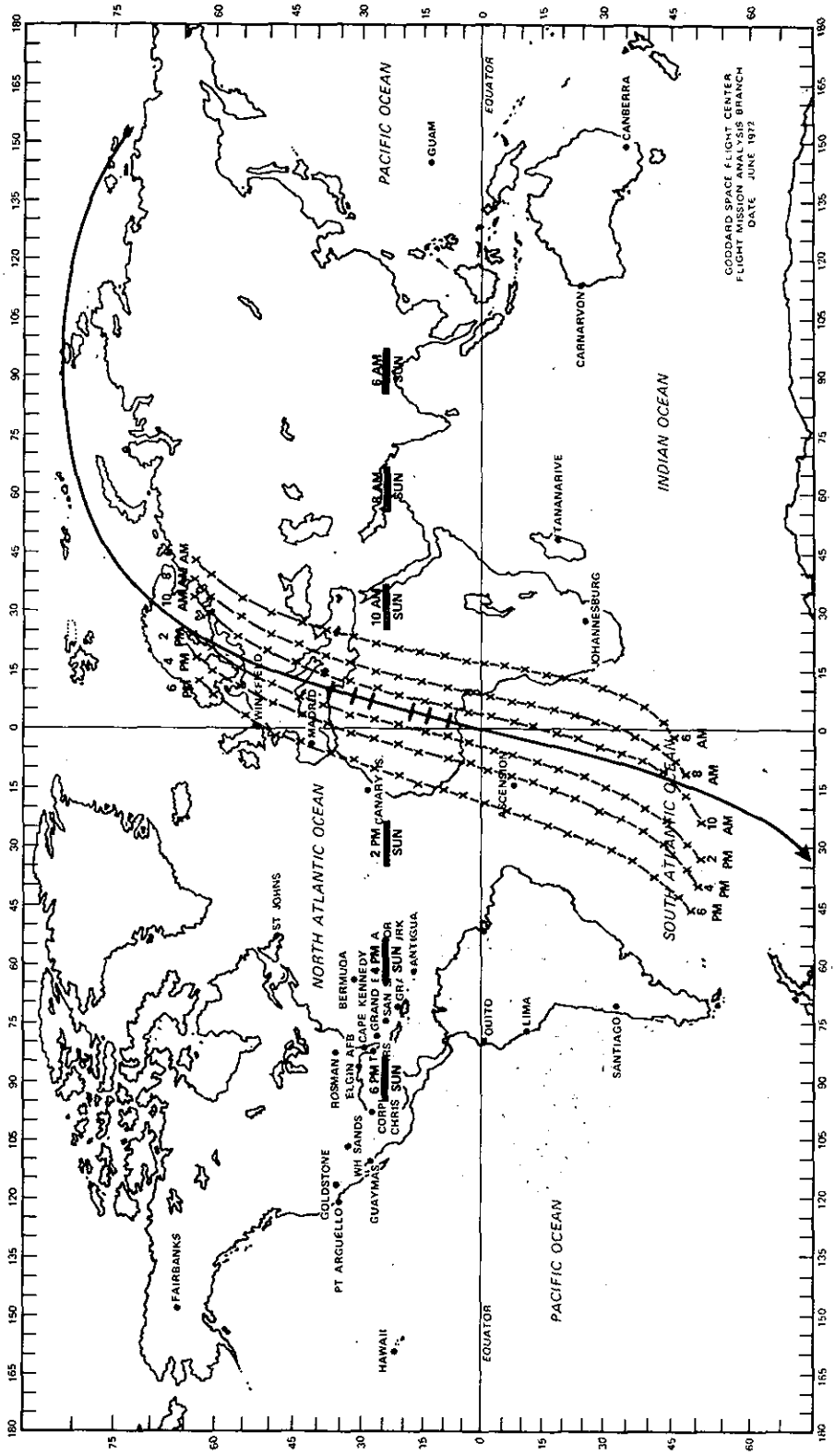

Figure 26. Glint Trace - Descending Nodes, Summer Solstice

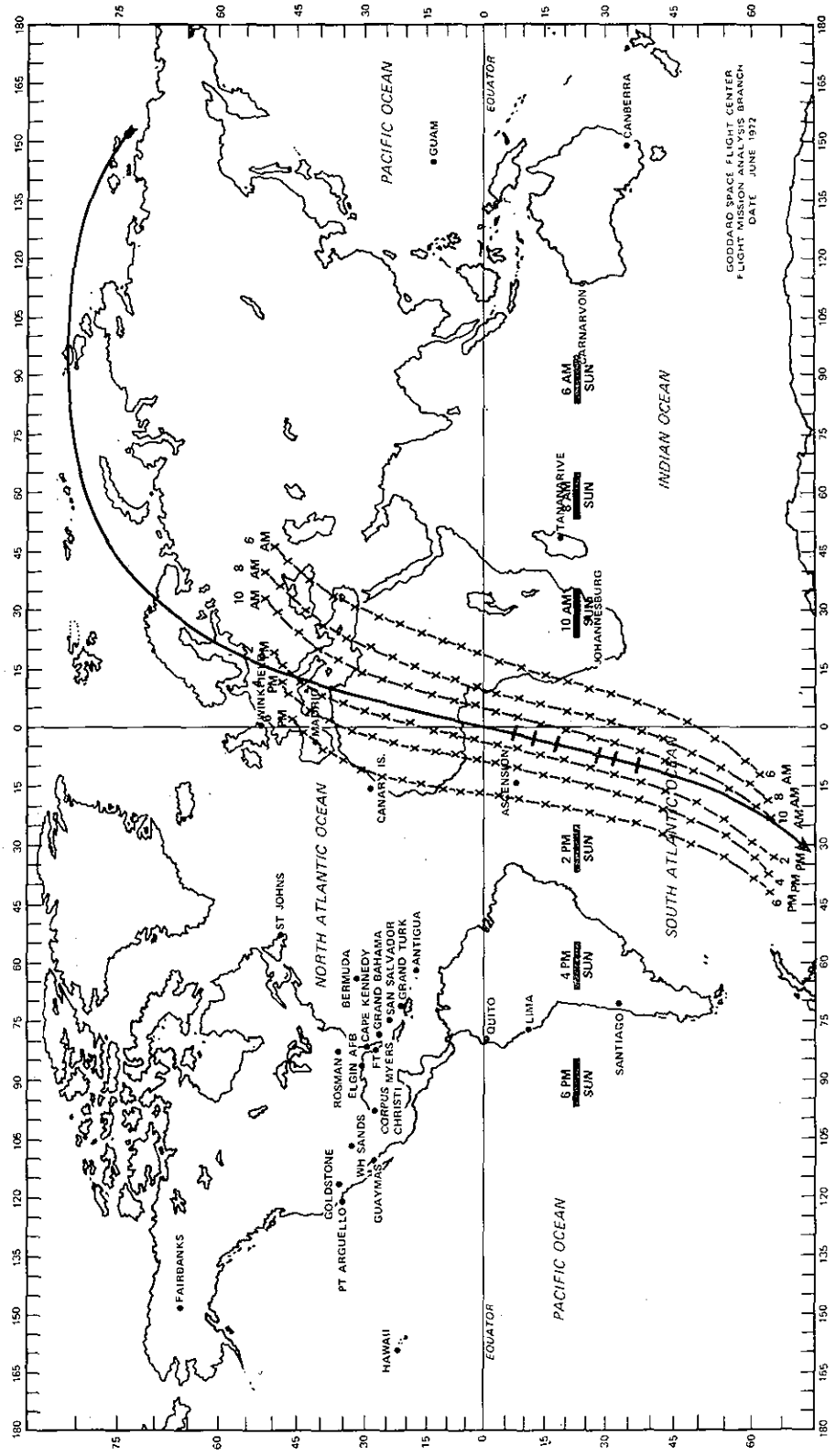

Figure 27. Glint Trace - Descending Nodes, Winter Solstice

CONCLUSIONS

For a sensor (such as a thematic mapper, oceanic imaging spectrophotometer, or radiometer) onboard an Earth observatory satellite (in a sun-synchronous orbit with approximately 976 km altitude) viewing along a line perpendicular to the subsatellite ground track, the extent of the ground coverage depends on the sensor width angle. A sensor width angle of 5 degrees gives a ground coverage half-angle of about 0.8 degrees, of 30 degrees gives a half-angle of 5.2 degrees, of 52 degrees gives a half-angle of 13.3 degrees, and a sensor able to view to the horizon has a ground coverage half-angle of 29.8 degrees. Thus a horizon sensor has a large viewing region and thus has a large variation in sensor illumination (i.e., sun elevation angle) from one end of the sensor ground coverage to the other. The sensor illumination is nearly symmetric (the same sun elevation angle at a point on one side of the coverage as for the corresponding point on the other side) for noon orbits. However, for 6 A.M. and 6 P.M. orbits, one end of the horizon and 30 degree sensor ground coverage is nearly always in sunlight during the course of the year while the other end is nearly always in darkness. Other orbits, 8 A.M., 10 A.M., 2 P.M., and 4 P.M., are also non-symmetric in their sensor illumination.

There are certain points, called "glint" points, where the sun's rays reflect off a smooth surface and into the spacecraft. For a 10 A.M. or 2 P.M. orbit the glint points occur near the ends of the 30 degree sensor, for an 8 A.M. or 4 P.M. orbit they occur between the ends of the 30 degree and 52 degree sensors, and for a 6 A.M. or 6 P.M. orbit they occur between the ends of the 52 degree and horizon sensors. Depending upon the orbit, a line sensor viewing perpendicular to the ground trace could look directly at a glint point somewhere between a subsatellite latitude of 38-1/2 degrees south and 38-1/2 degrees north.

ACKNOWLEDGEMENT

The author wishes to acknowledge helpful discussions with Mr. Wilber B. Huston, Earth Observatory Satellite (EOS) Study Manager, who pointed out and discussed the effect of the sensor illumination and the glint point problem on sensor development and selection.

REFERENCES

1. Cooley, J. L., "Orbit Selection Considerations for Earth Observatory Satellites," X-551-72-145, April 1972.

2. SANDTRACKS World Map and Look Angles Computer Program, GSFC program number D00101, GSFC computer program library.

3. Orbital Flight Handbook, Volume I, Part 3 -- Requirements, Prepared for the George C. Marshall Space Flight Center, 1963, pages XIII-17 to XIII-22.